Electronic Supplementary Information

for

Substrate-Product Analogue Inhibitors Isoleucine 2-Epimerase from *Lactobacillus buchneri* by Rational Design†

Noa T. Sorbara[1], Joshua W.M. MacMillan[2], Gregory D. McCluskey[1], and Stephen L. Bearne[1,2,*]

[1] Department of Biochemistry & Molecular Biology, Dalhousie University, Halifax, Nova Scotia, B3H 4R2, Canada

[2] Department of Chemistry, Dalhousie University, Halifax, Nova Scotia, B3H 4R2, Canada

† This work was supported by a Discovery Grant from the Natural Sciences and Engineering Research Council (NSERC) of Canada (S.L.B.) and NSERC-USRAs (N.T.S. and J.W.M.M.).

* Author to whom correspondence should be addressed.
Phone: (902) 494-1974; fax: (902) 494-1355; e-mail: sbearne@dal.ca

TABLE OF CONTENTS **PAGE**

Figure S1. ^{1}H NMR spectrum of 3-ethyl-L-norvaline (**6a**)

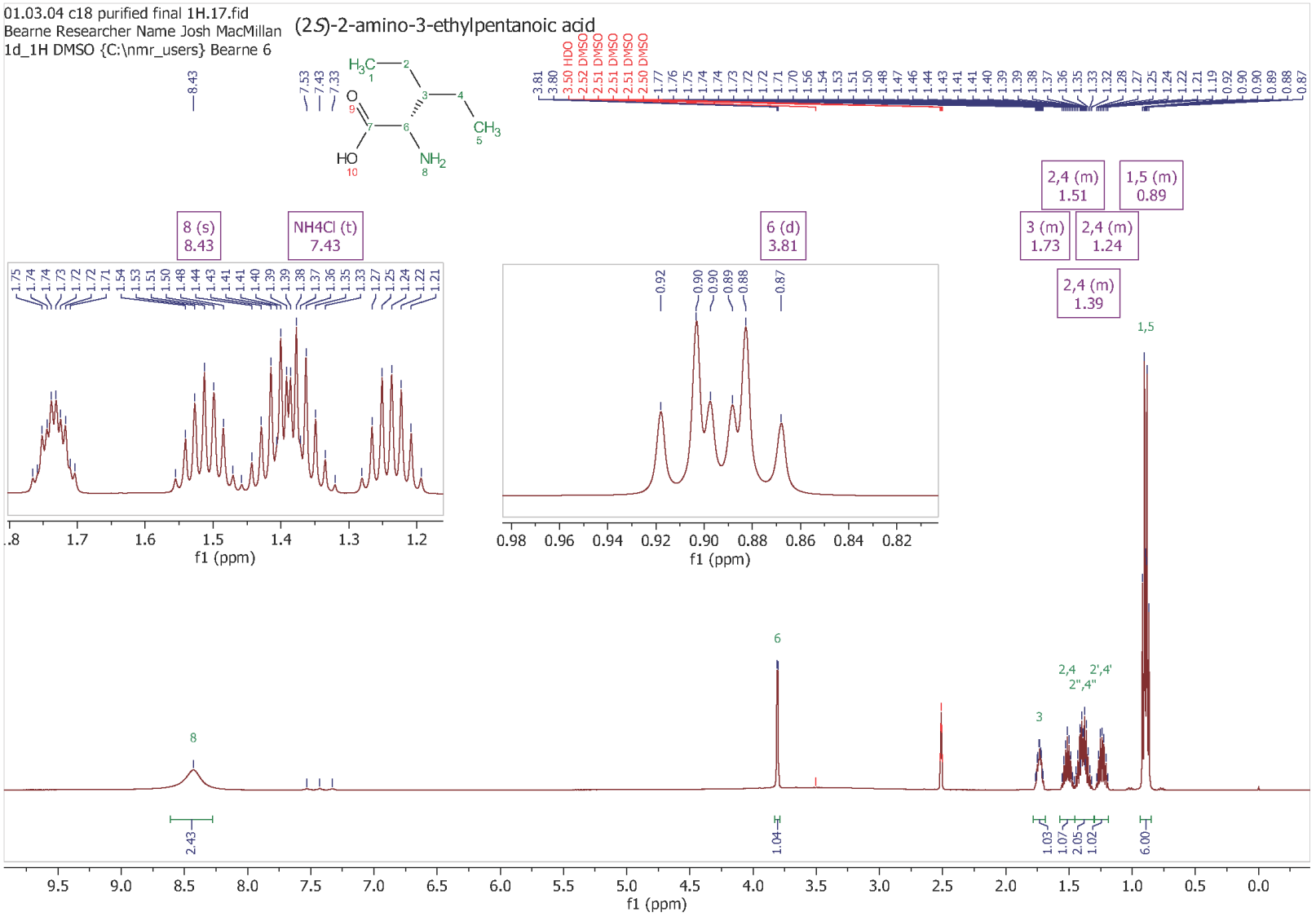

Figure S1

Figure S2. ^{13}C NMR spectrum of 3-ethyl-L-norvaline (**6a**)

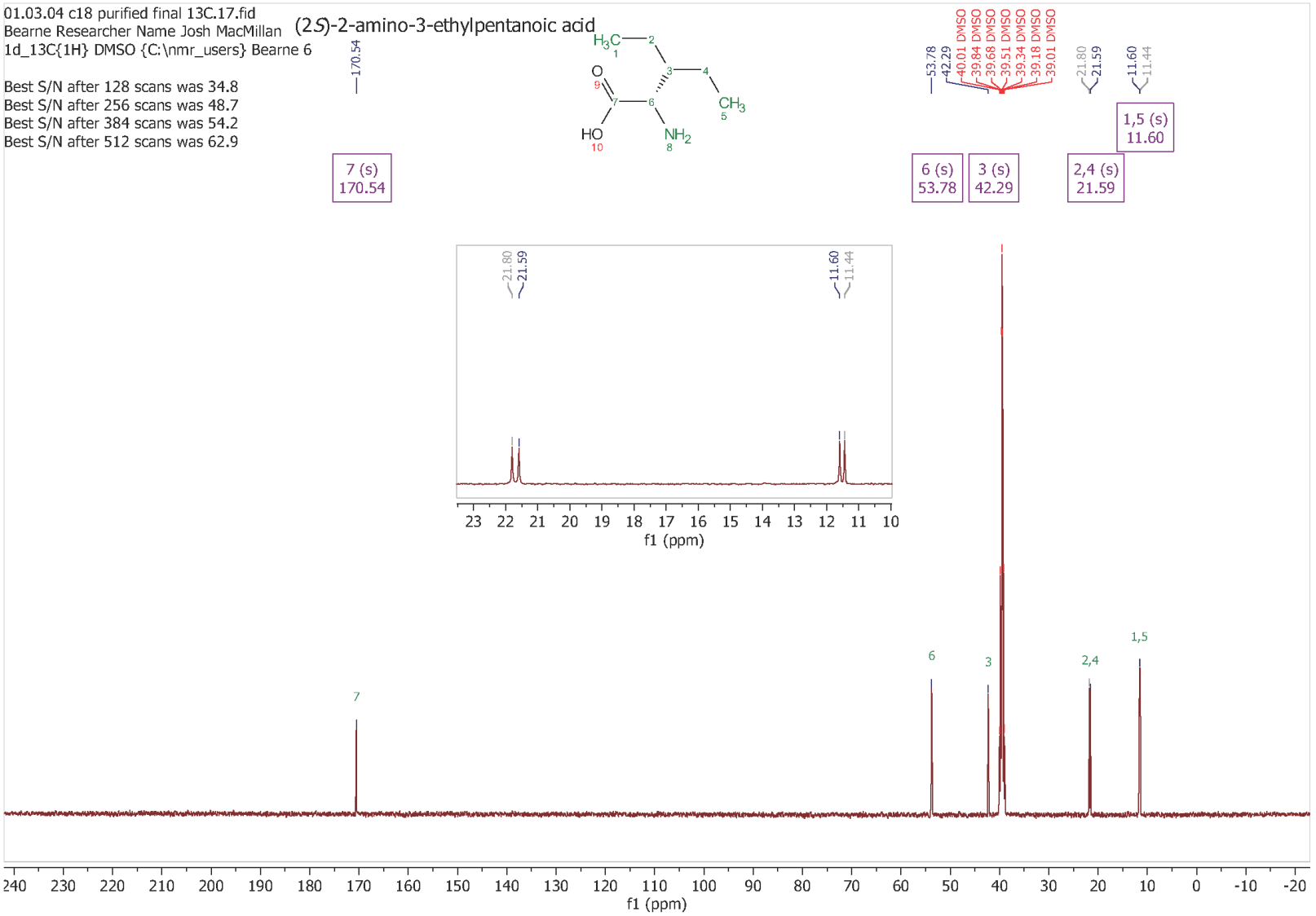

Figure S2

Figure S3. ^{1}H NMR spectrum of (2*S*)-3-ethyl-3-methyl-2-{[(1*S*)-1-phenylethyl]amino}pentanenitrile (**2b**)

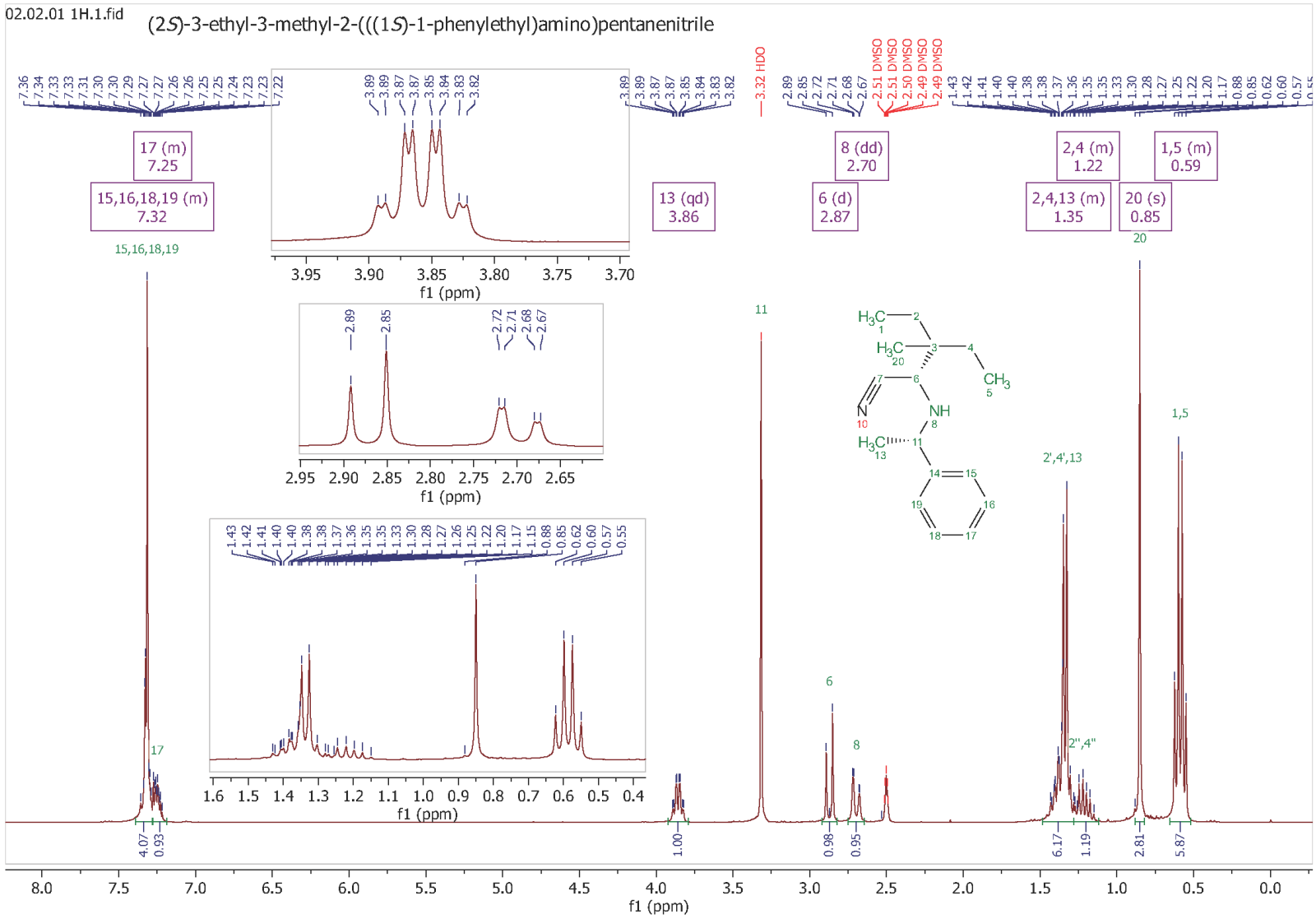

Figure S3

Figure S4. ^{13}C NMR spectrum of (2*S*)-3-ethyl-3-methyl-2-{[(1*S*)-1-phenylethyl]amino}pentanenitrile (**2b**)

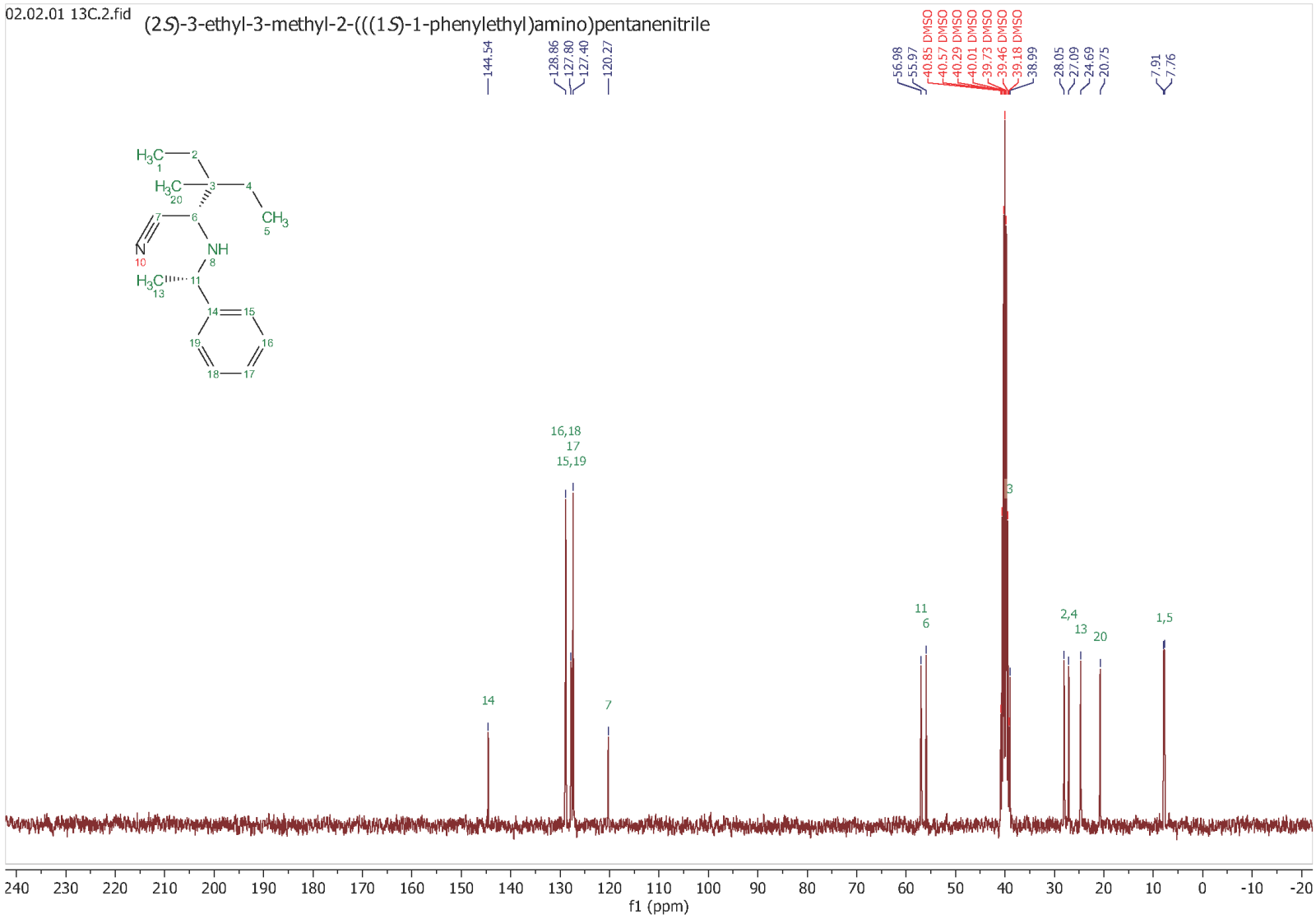

Figure S4

Figure S5. ^{1}H NMR spectrum of 3-ethyl-3-methyl-N^{2}-[(1*S*)-1-phenylethyl]-L-norvalinamide (**4b**)

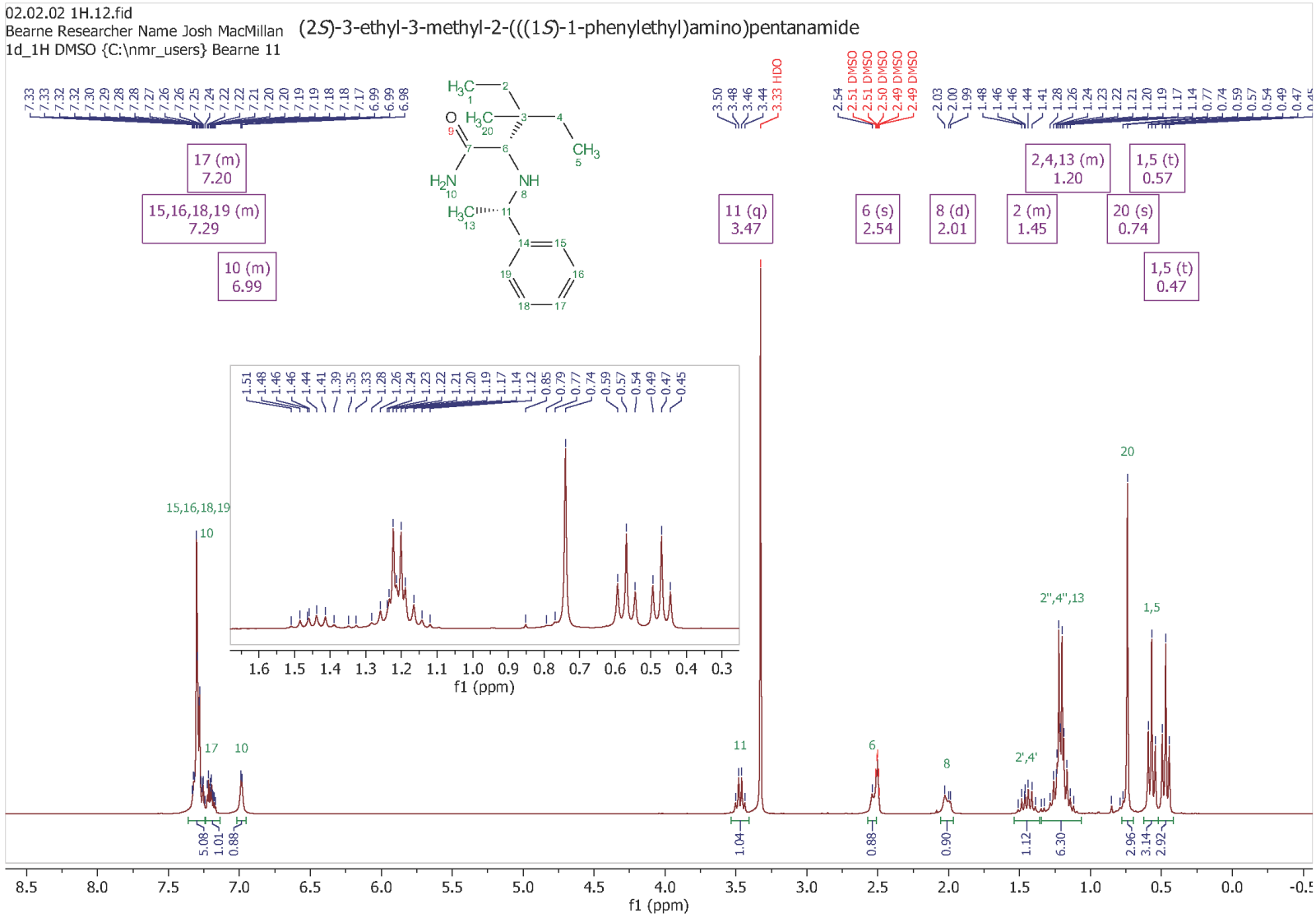

Figure S5

Figure S6. ^{13}C NMR spectrum of 3-ethyl-3-methyl-N^2-[(1*S*)-1-phenylethyl]-L-norvalinamide (**4b**)

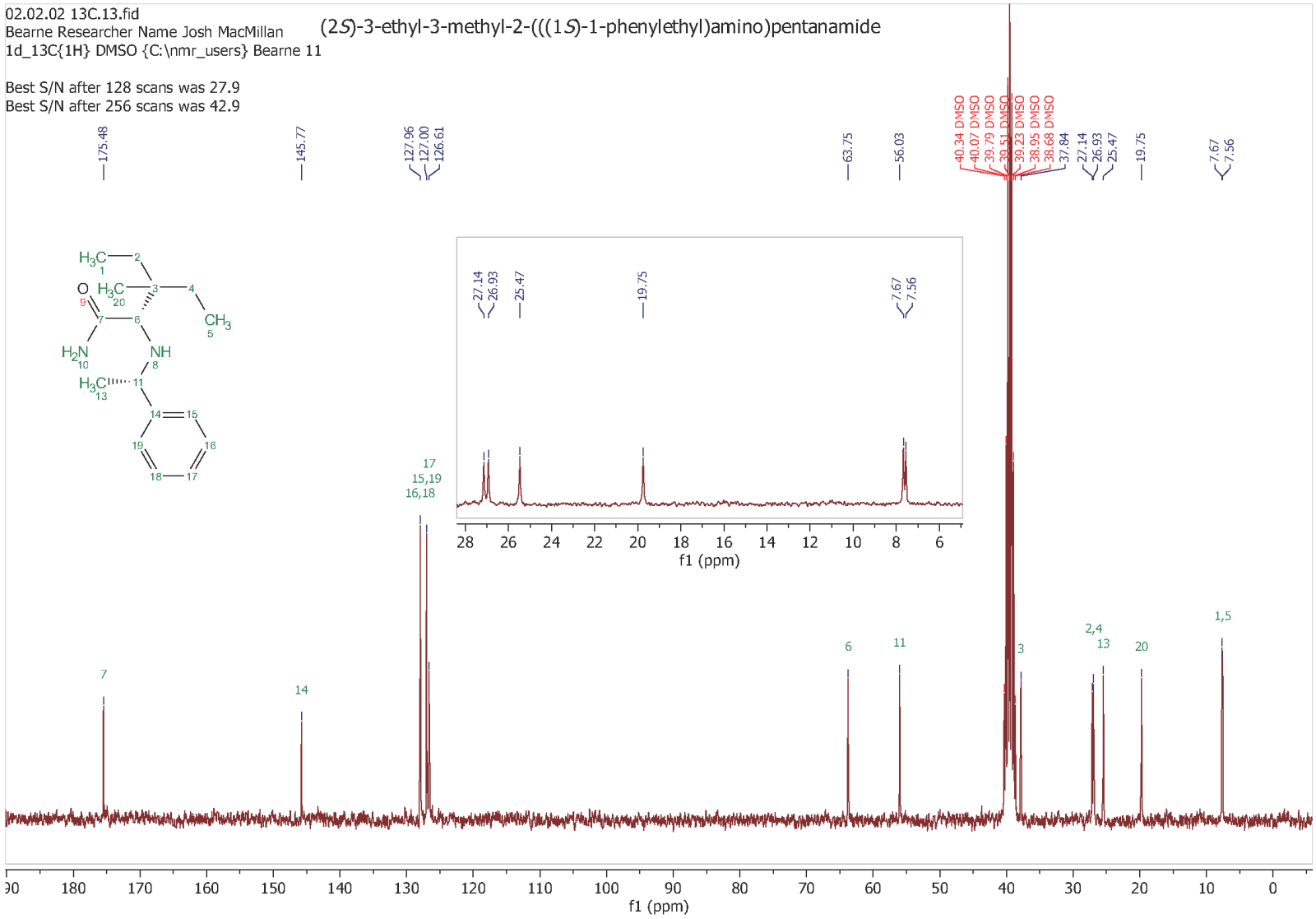

Figure S6

Figure S7. ^{1}H NMR spectrum of 3-ethyl-3-methyl-L-norvalinamide (**5b**)

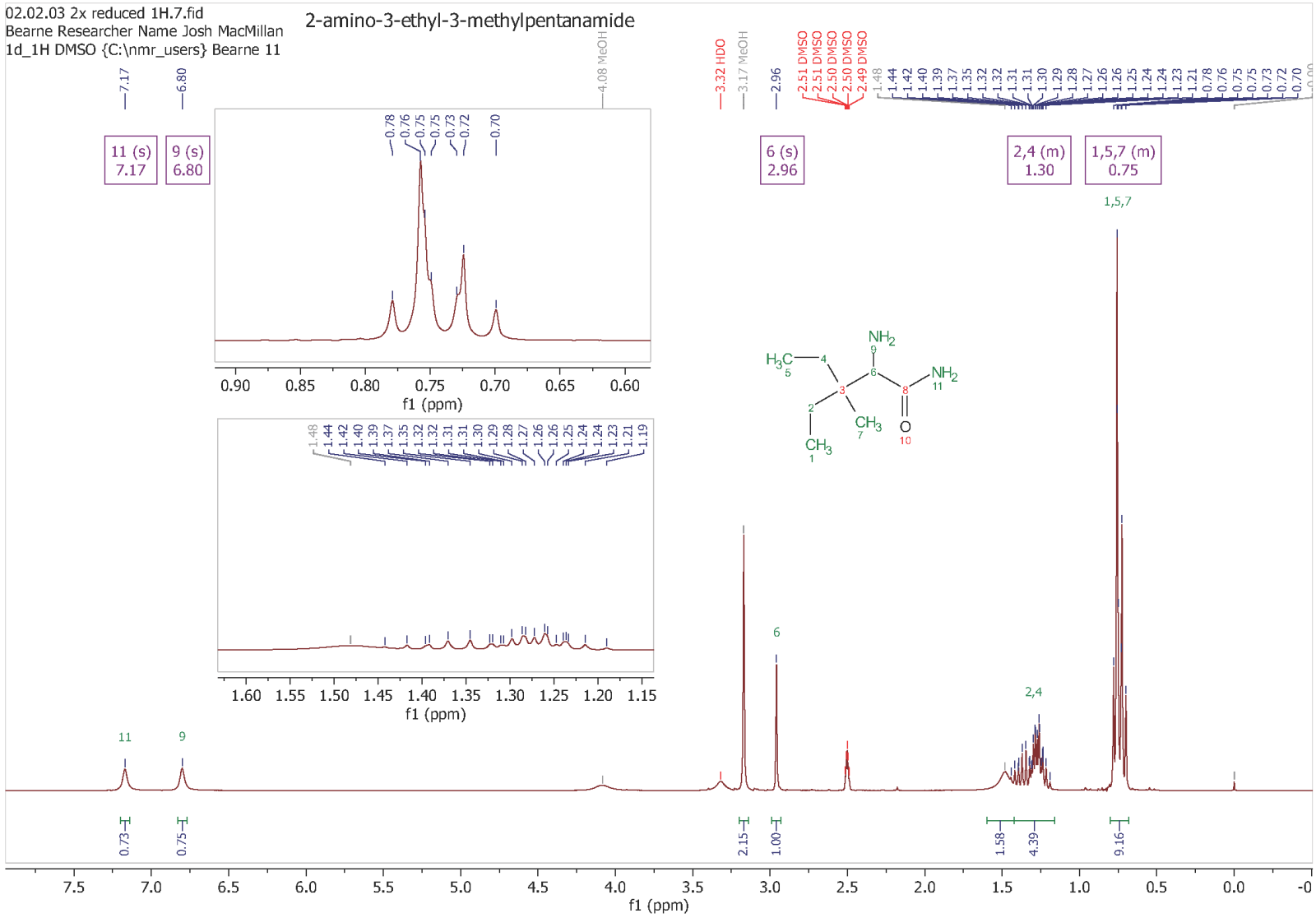

Figure S7

Figure S8. ^{13}C NMR spectrum of 3-ethyl-3-methyl-L-norvalinamide (**5b**)

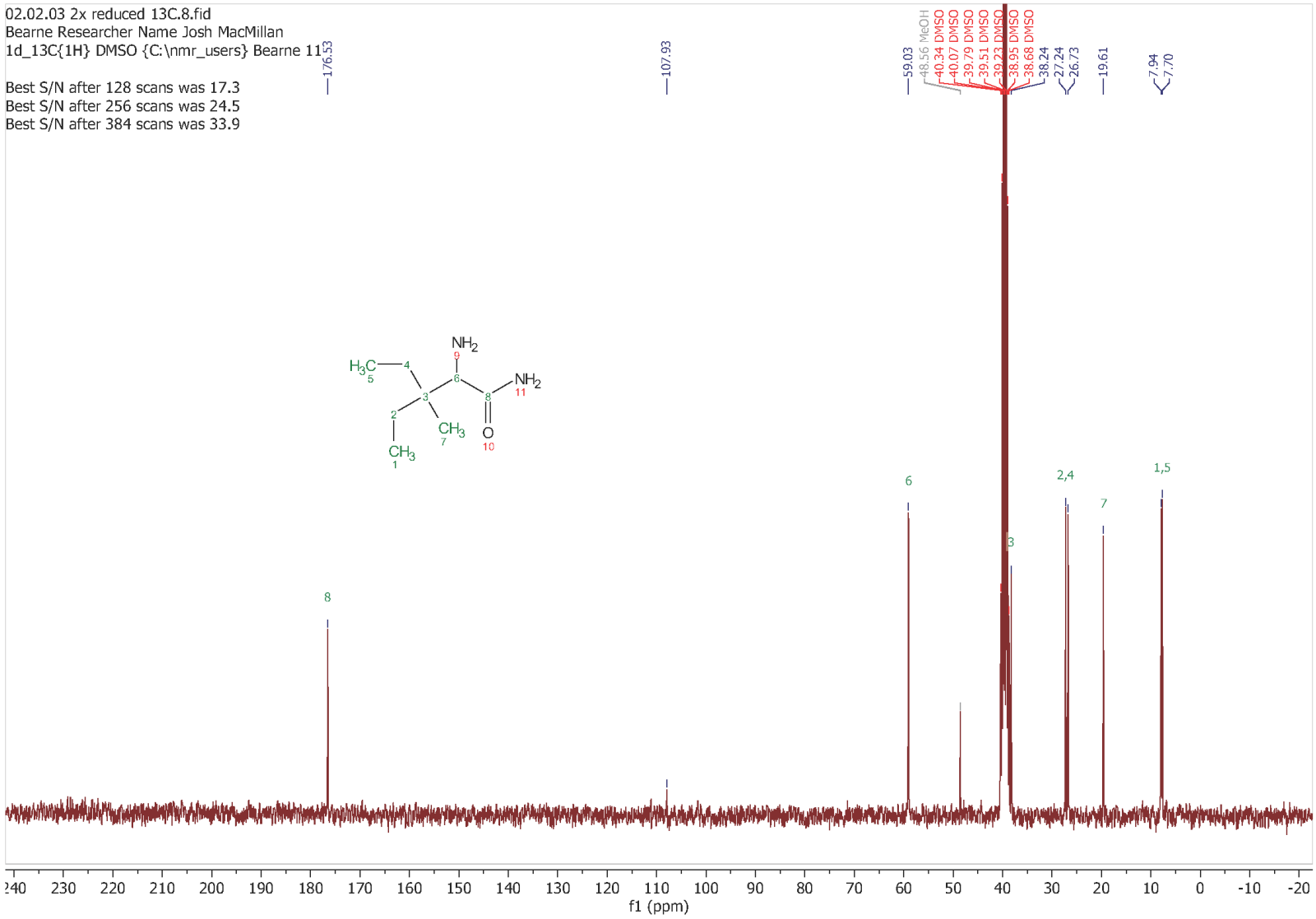

Figure S8

Figure S9. ^{1}H NMR spectrum of 3-ethyl-3-methyl-L-norvaline (**6b**)

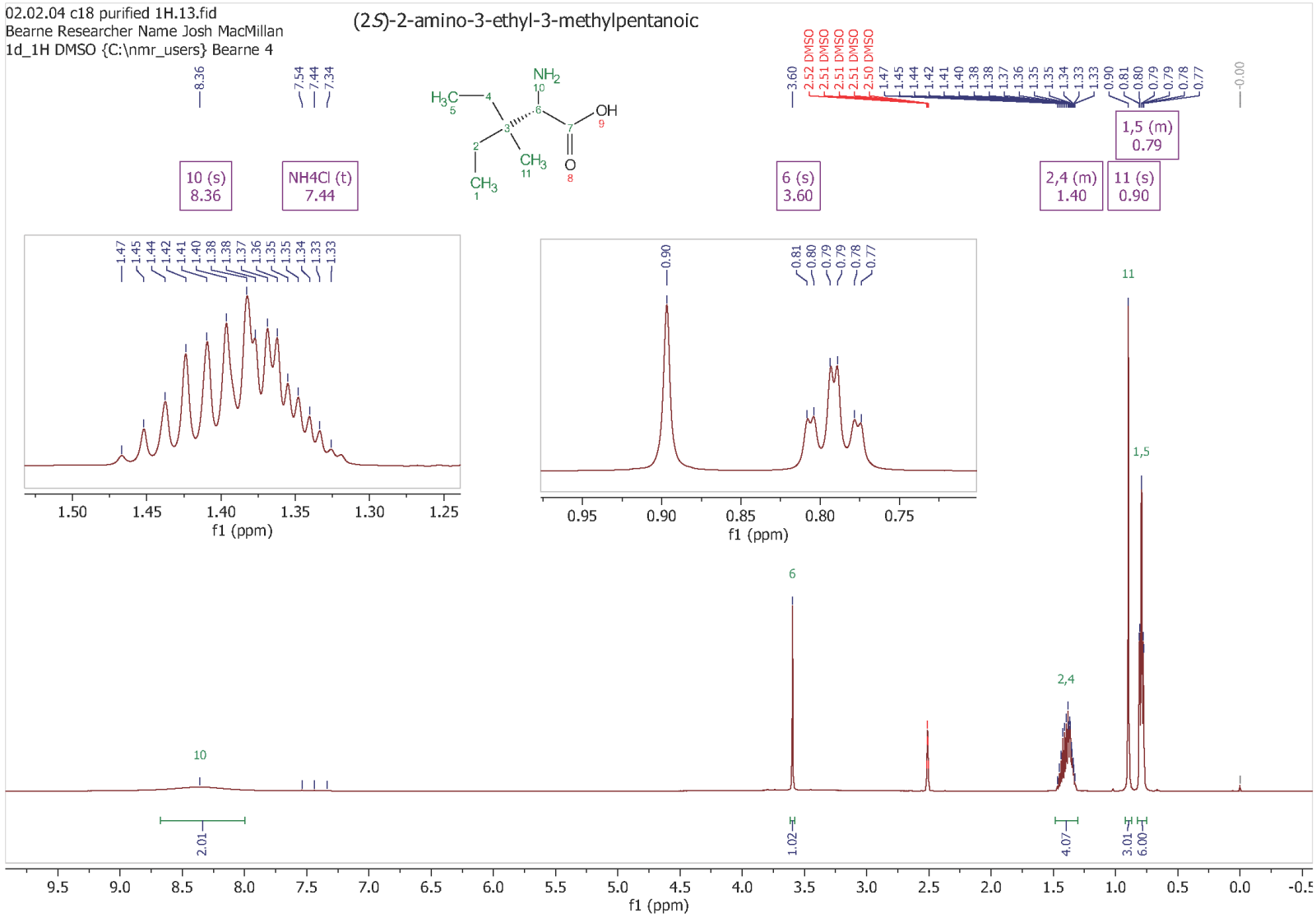

Figure S9

Figure S10. ^{13}C NMR spectrum of 3-ethyl-3-methyl-L-norvaline (**6b**)

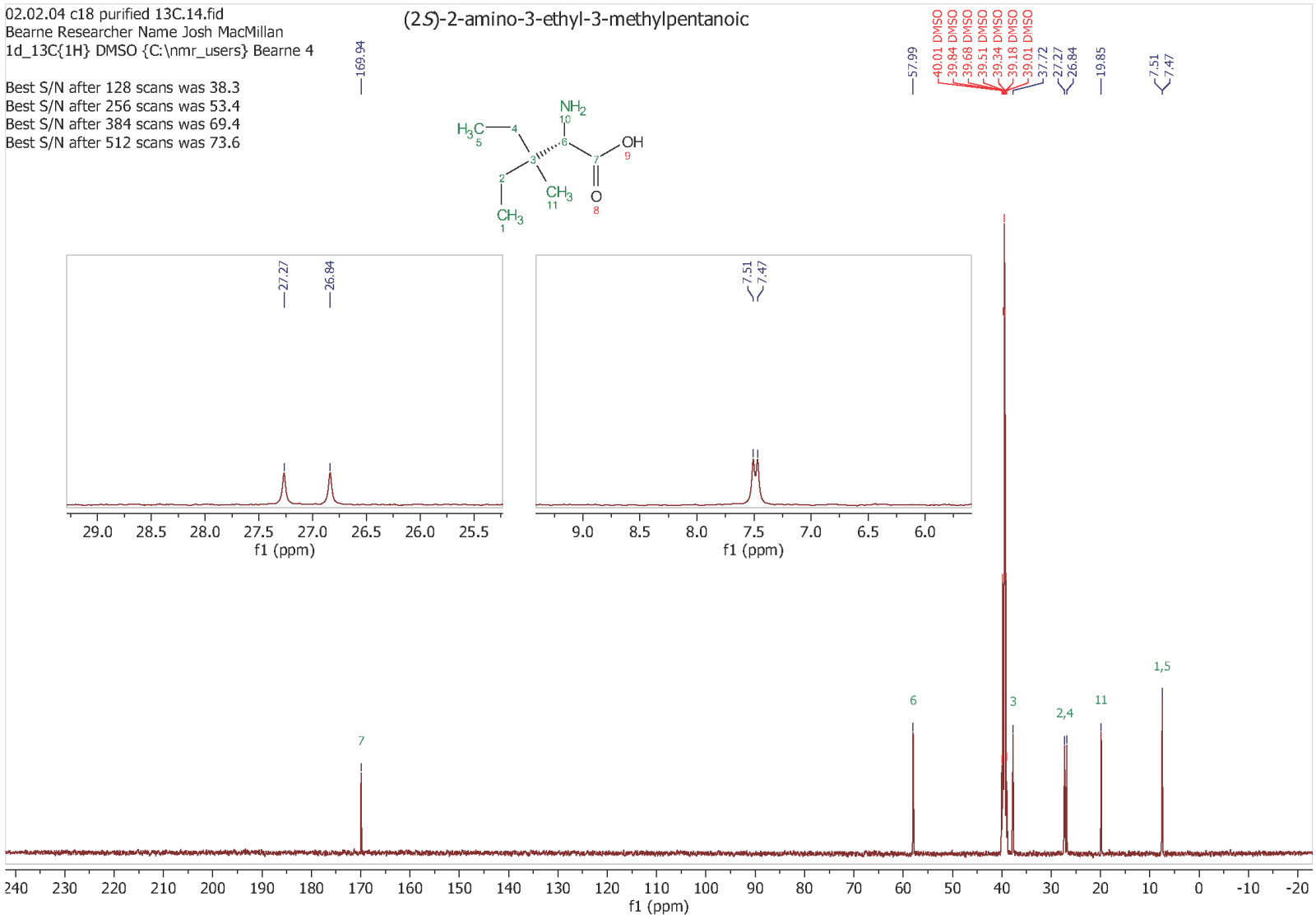

Figure S10

Figure S11. ^{1}H NMR spectrum of (2*R*)-3-ethyl-2-{[(1*R*)-1-phenylethyl]amino}pentanenitrile (**7a**)

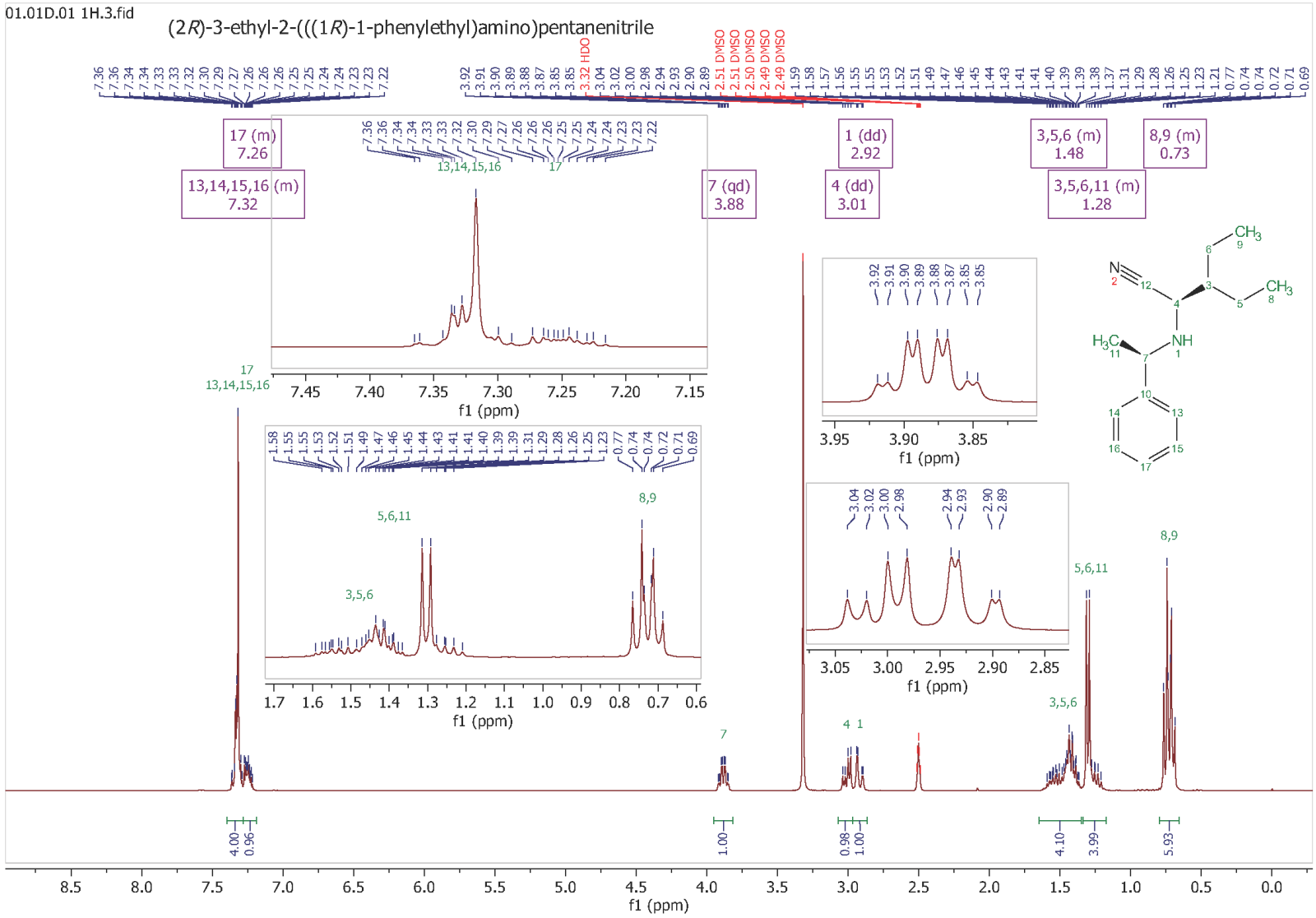

Figure S11

Figure S12. ^{13}C NMR spectrum of (2*R*)-3-ethyl-2-{[(1*R*)-1-phenylethyl]amino}pentanenitrile (**7a**)

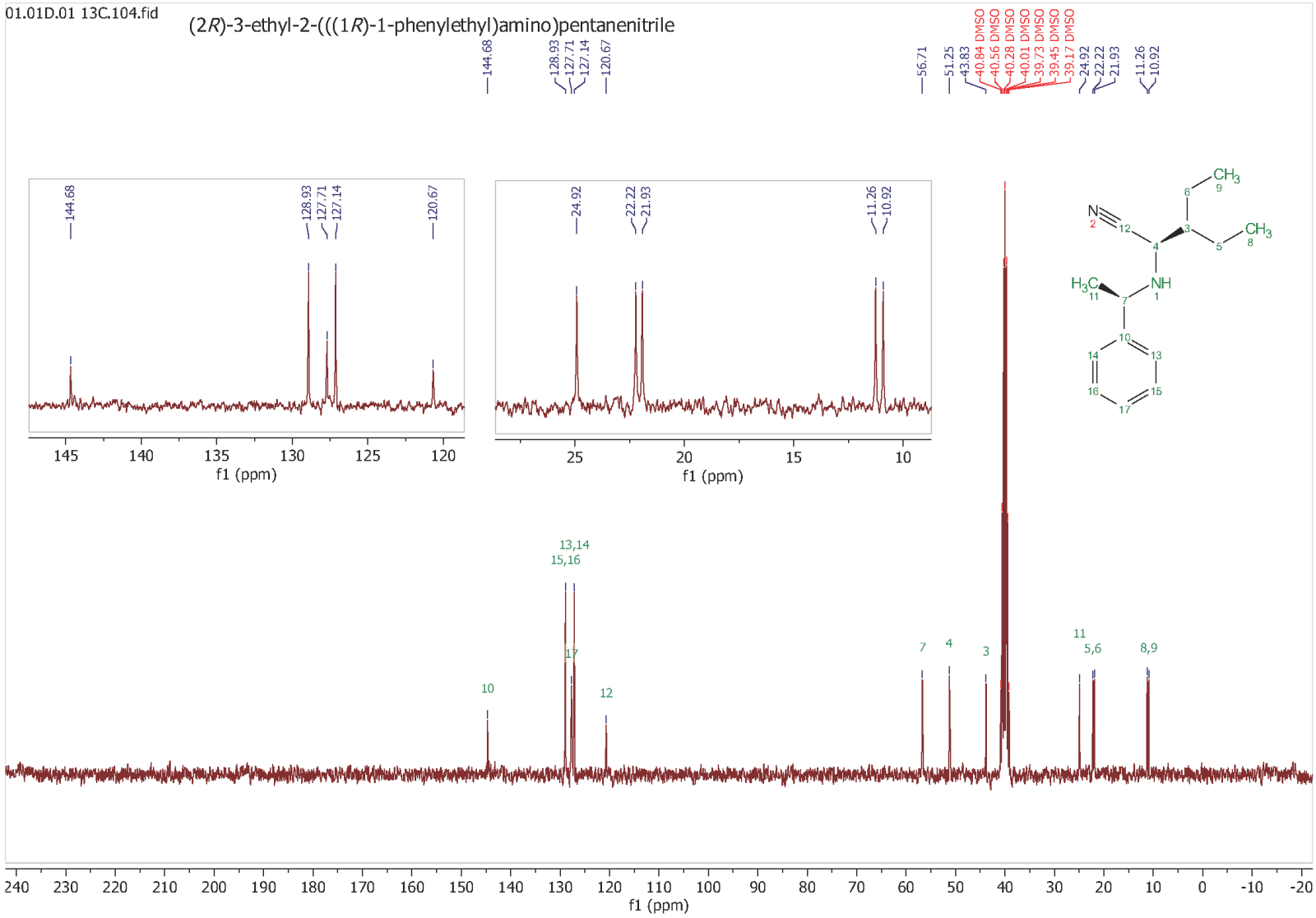

Figure S12

Figure S13. ^{1}H NMR spectrum of 3-ethyl-N^{2}-[(1*R*)-1-phenylethyl]-D-norvalinamide (**9a**)

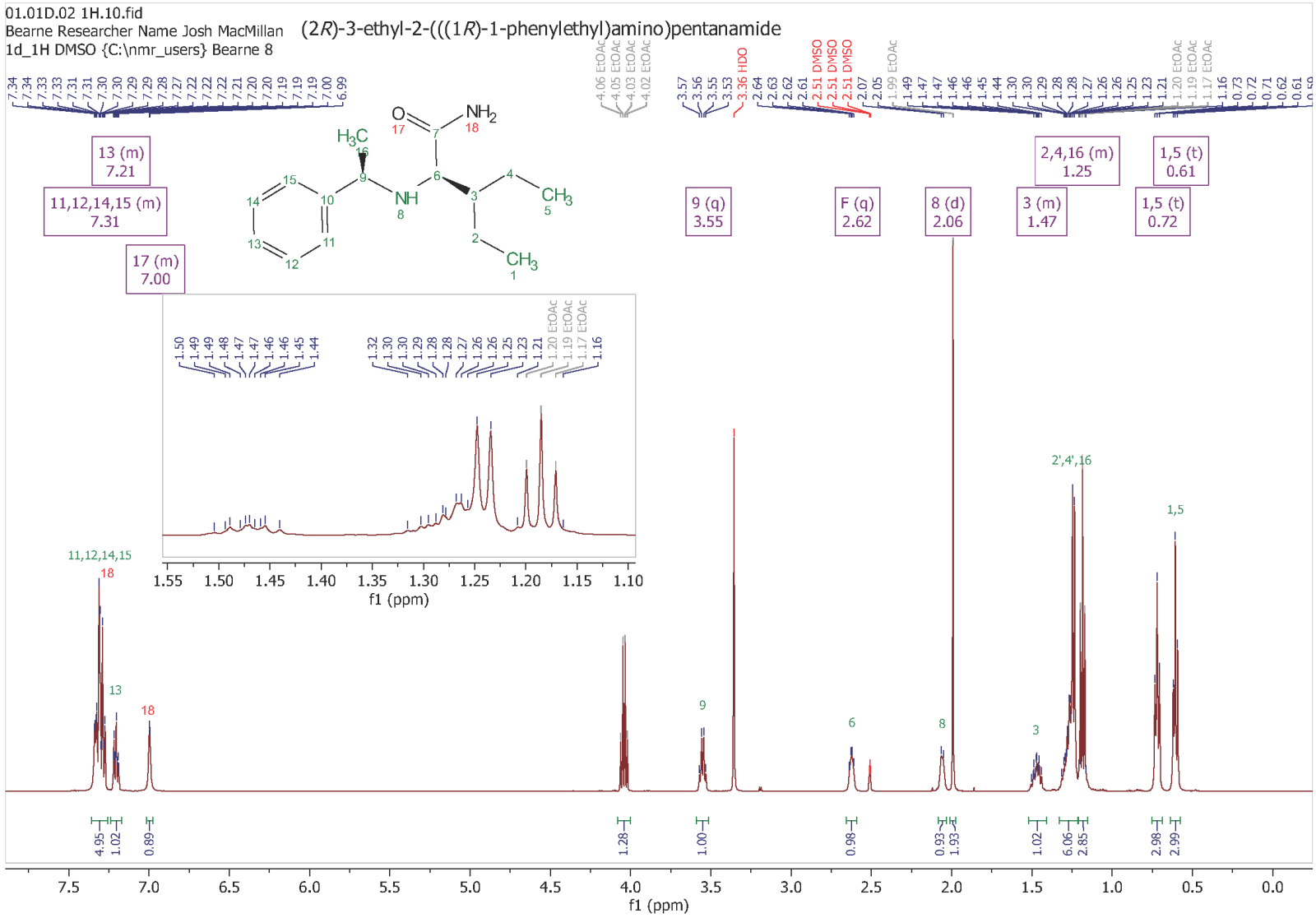

Figure S13

Figure S14. ^{13}C NMR spectrum of 3-ethyl-N^2-[(1*R*)-1-phenylethyl]-D-norvalinamide (**9a**)

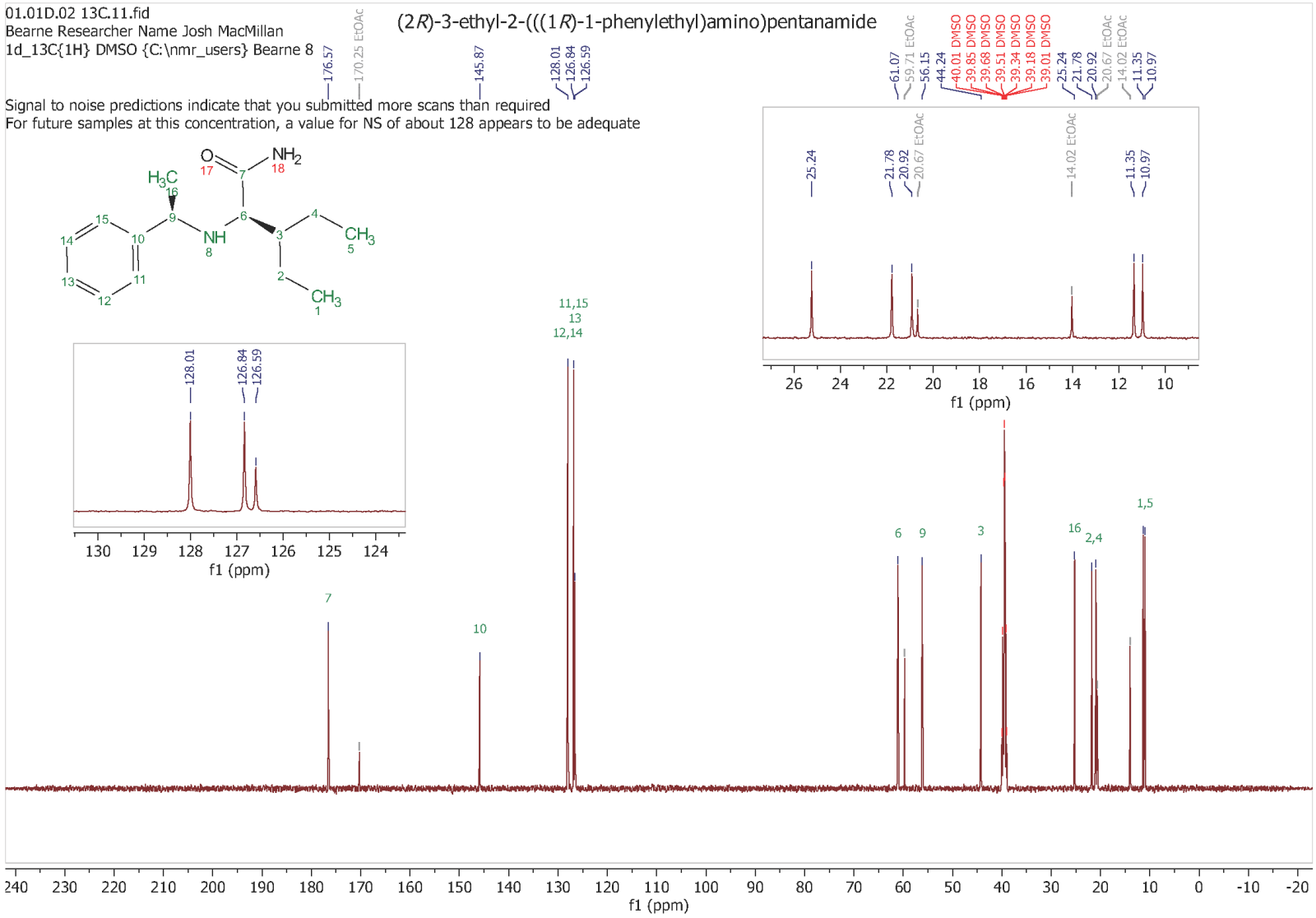

Figure S14

Figure S15. ^{1}H NMR spectrum of 3-ethyl-D-norvalinamide (**10a**)

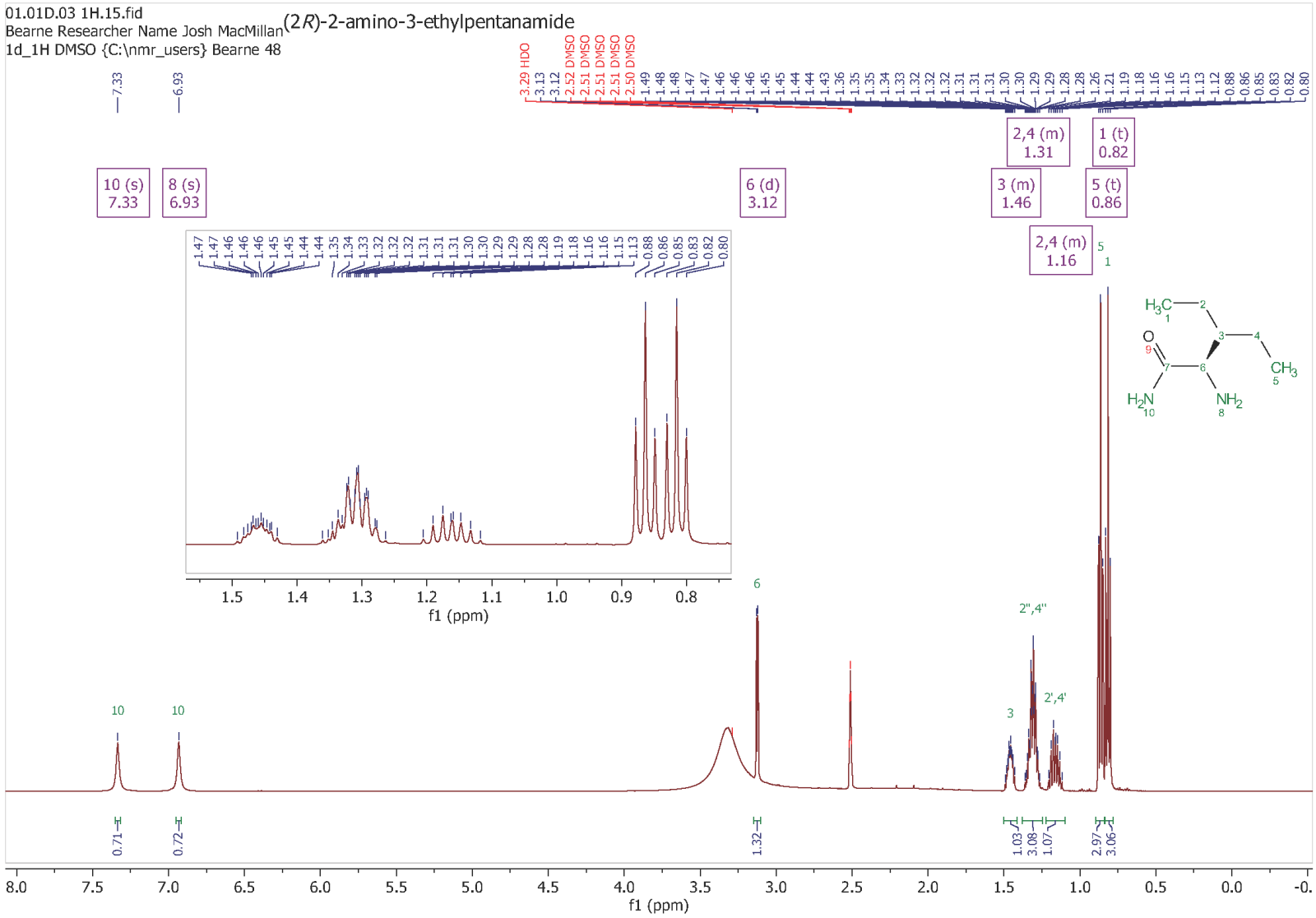

Figure S15

Figure S16. ^{13}C NMR spectrum of 3-ethyl-D-norvalinamide (**10a**)

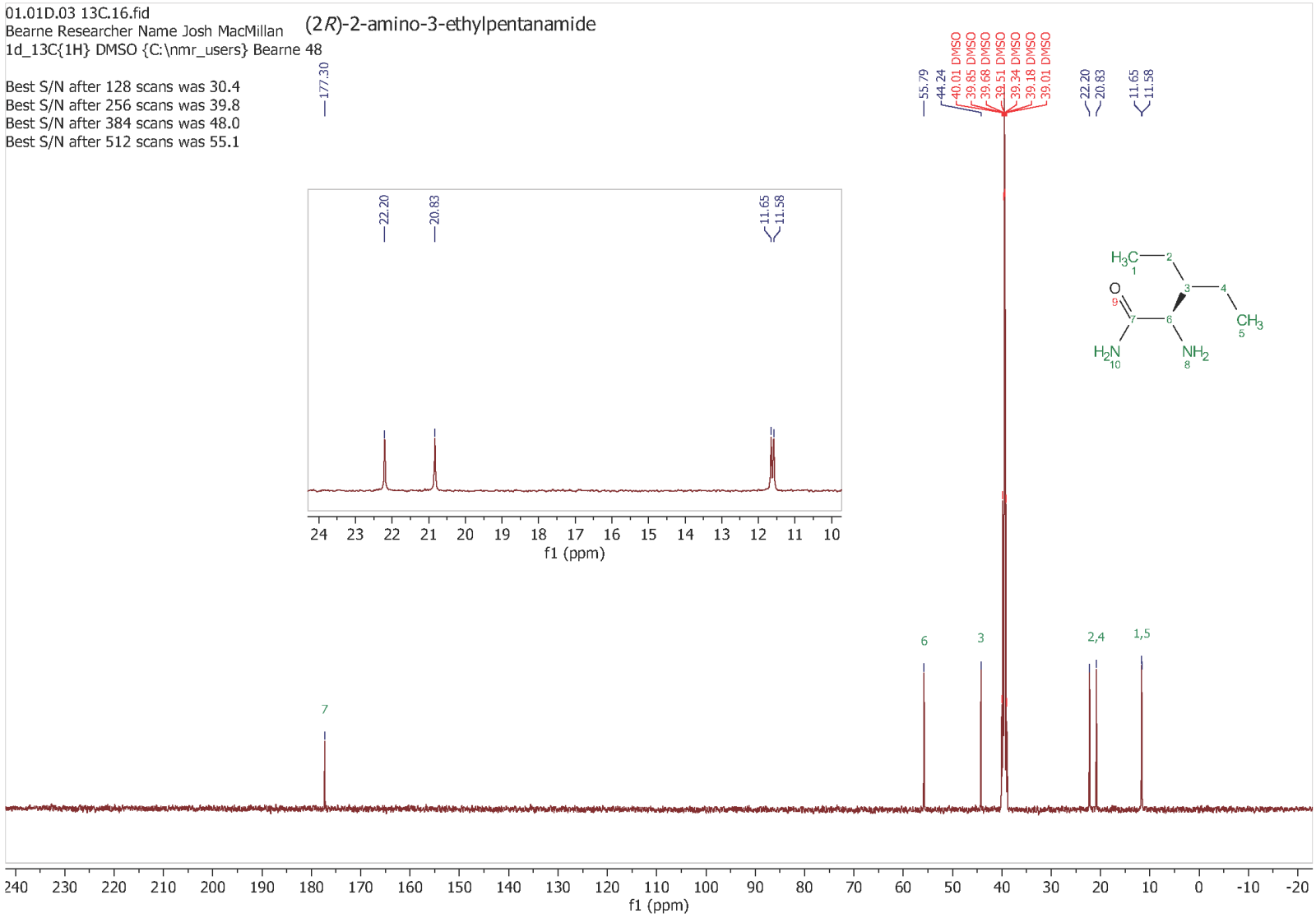

Figure S16

Figure S17. ^{1}H NMR spectrum of 3-ethyl-D-norvaline (**11a**)

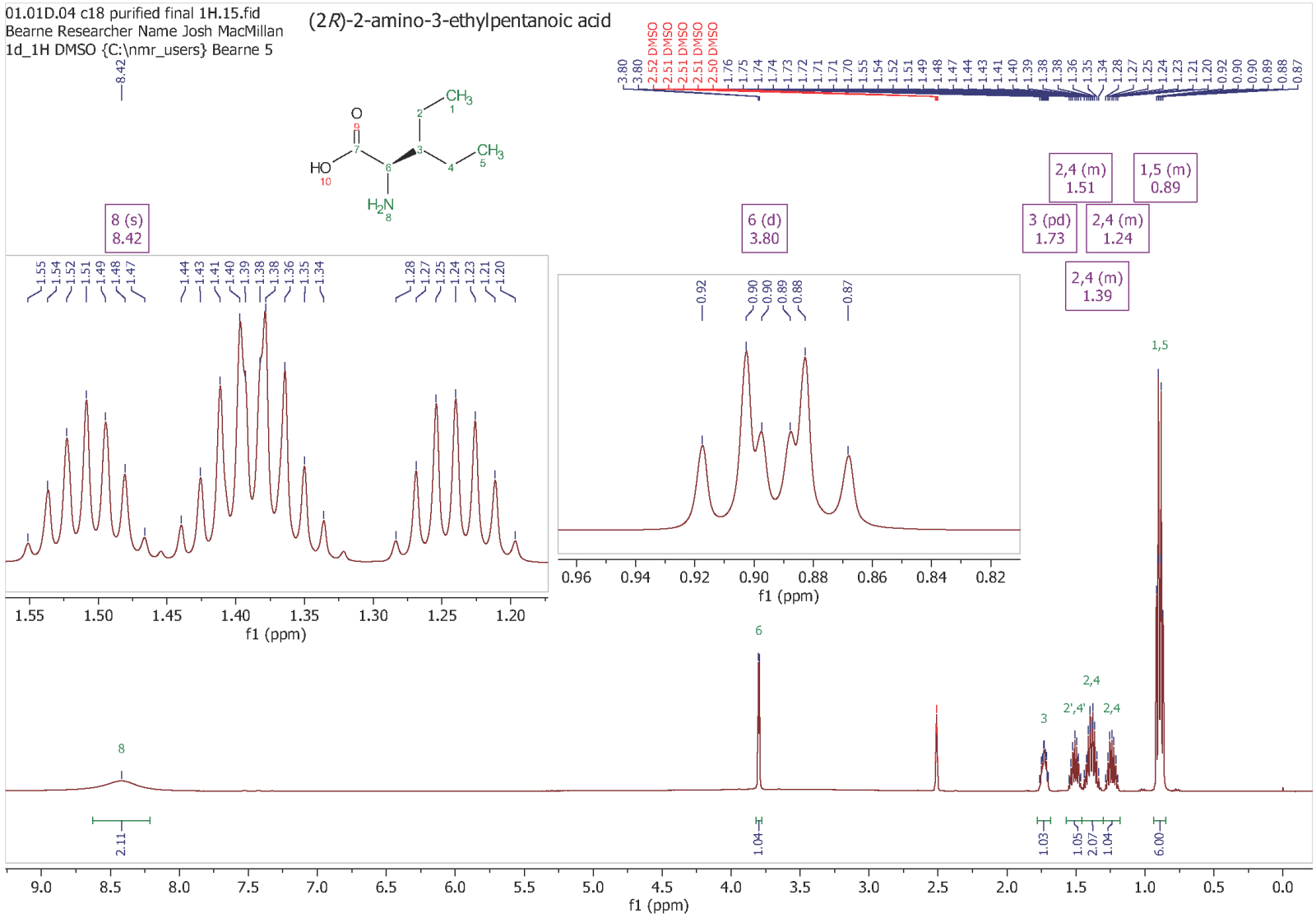

Figure S17

Figure S18. ^{13}C NMR spectrum of 3-ethyl-D-norvaline (**11a**)

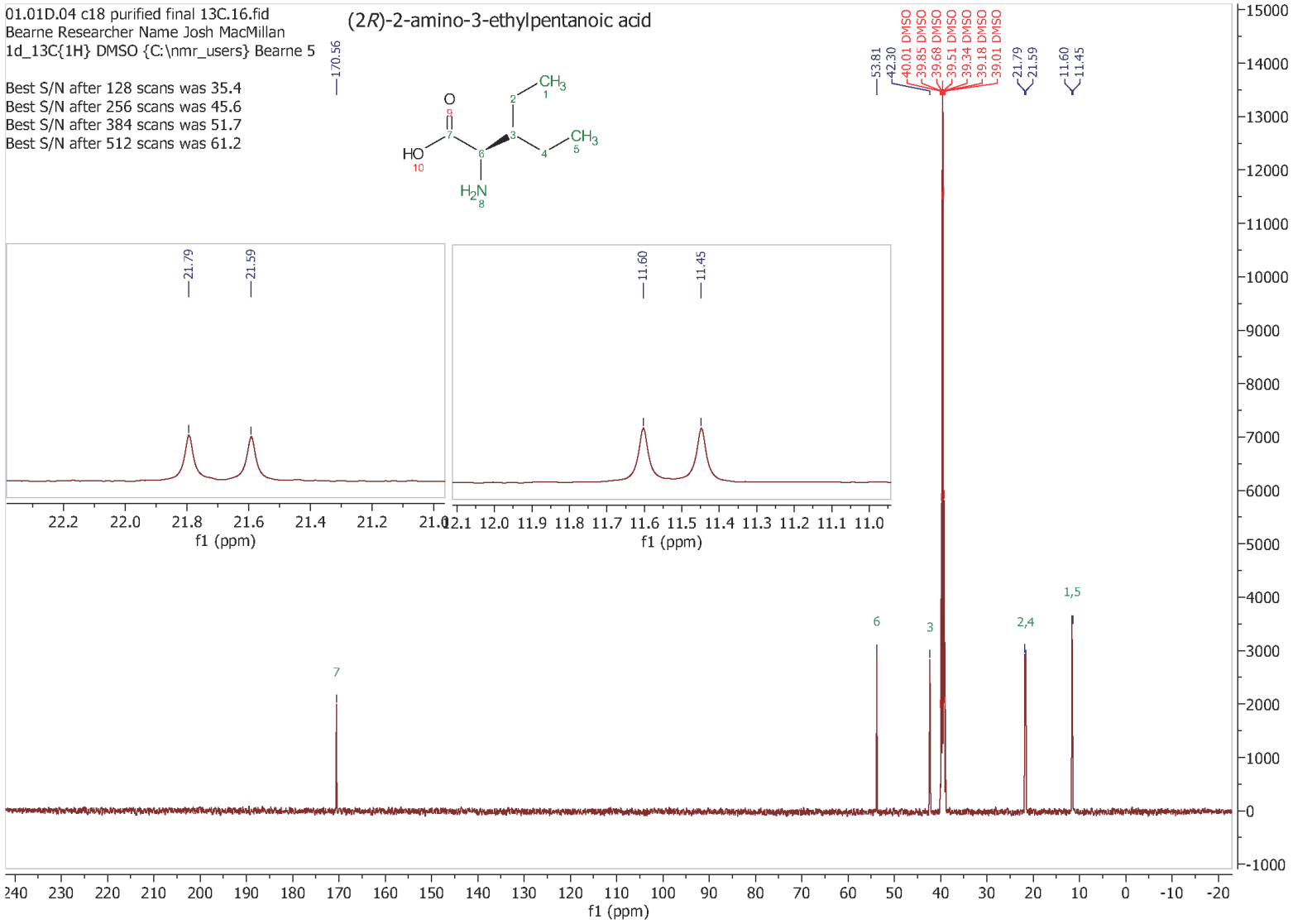

Figure S18

Figure S19. ^{1}H NMR spectrum of (2*R*)-3-ethyl-3-methyl-2-{[(1*R*)-1-phenylethyl]amino}pentanenitrile (**7b**)

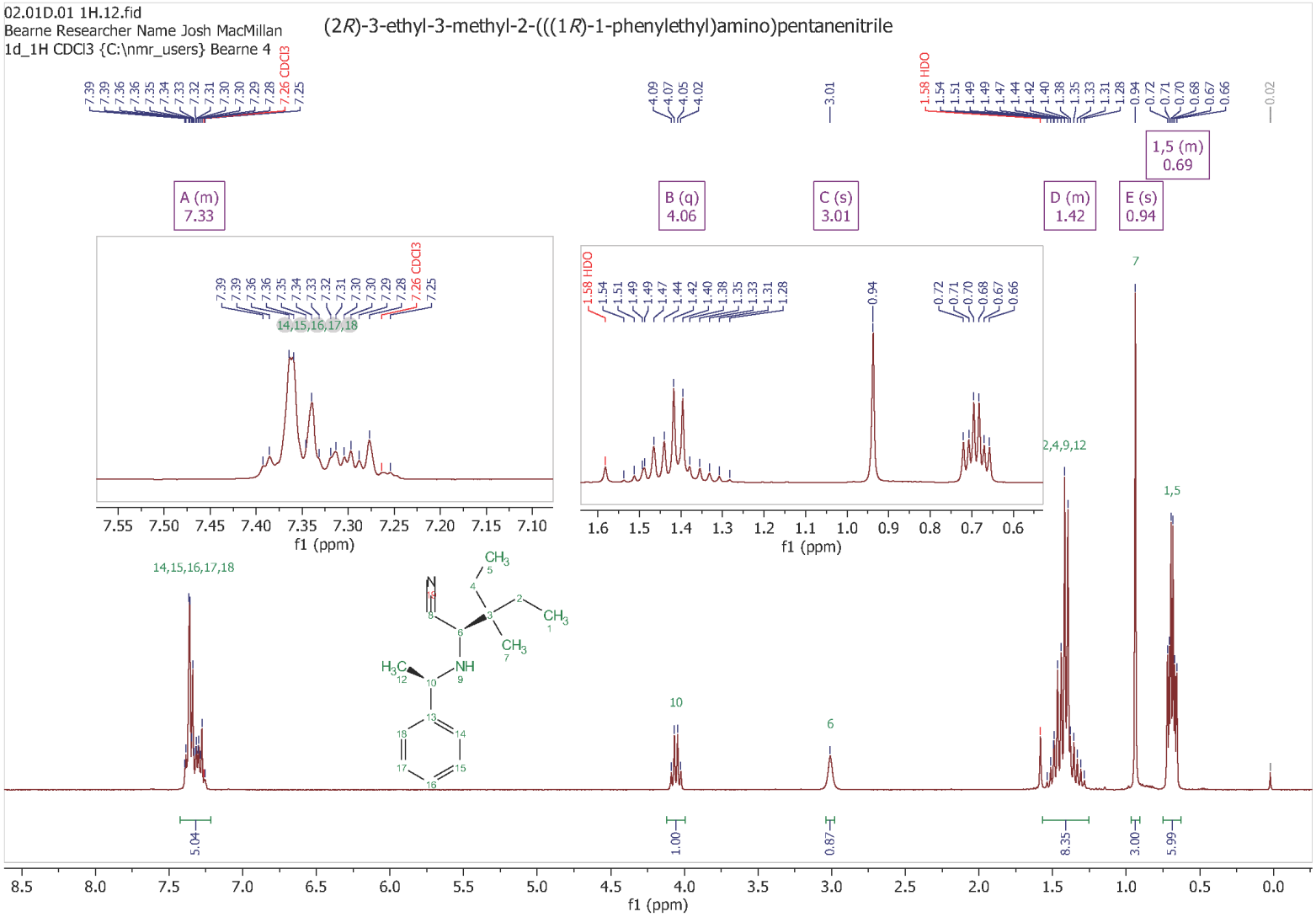

Figure S19

Figure S20. ^{13}C NMR spectrum of (2*R*)-3-ethyl-3-methyl-2-{[(1*R*)-1-phenylethyl]amino}pentanenitrile (**7b**)

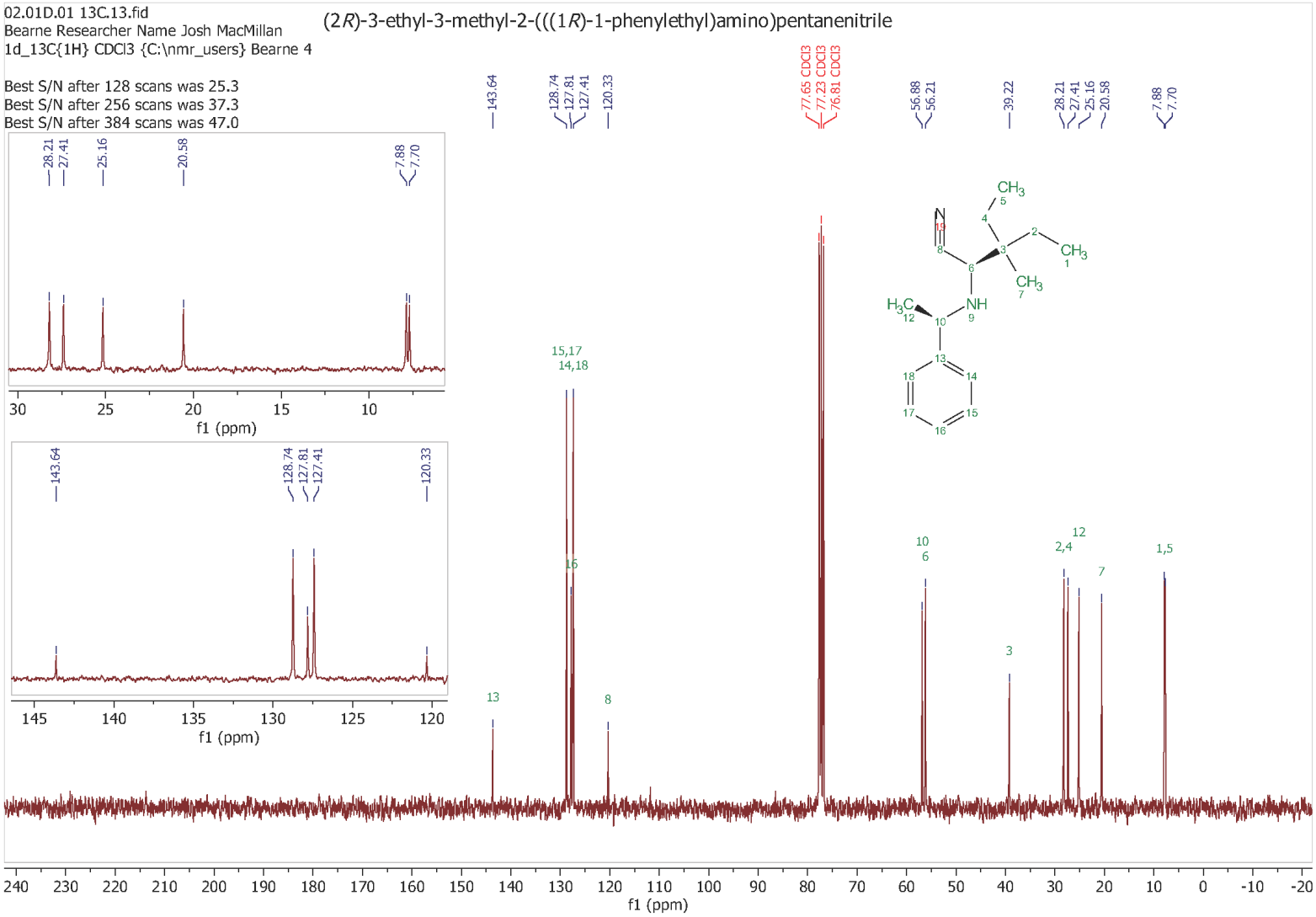

Figure S20

Figure S21. ^{1}H NMR spectrum of 3-ethyl-3-methyl-N^{2}-[(1*R*)-1-phenylethyl]-D-norvalinamide (**9b**)

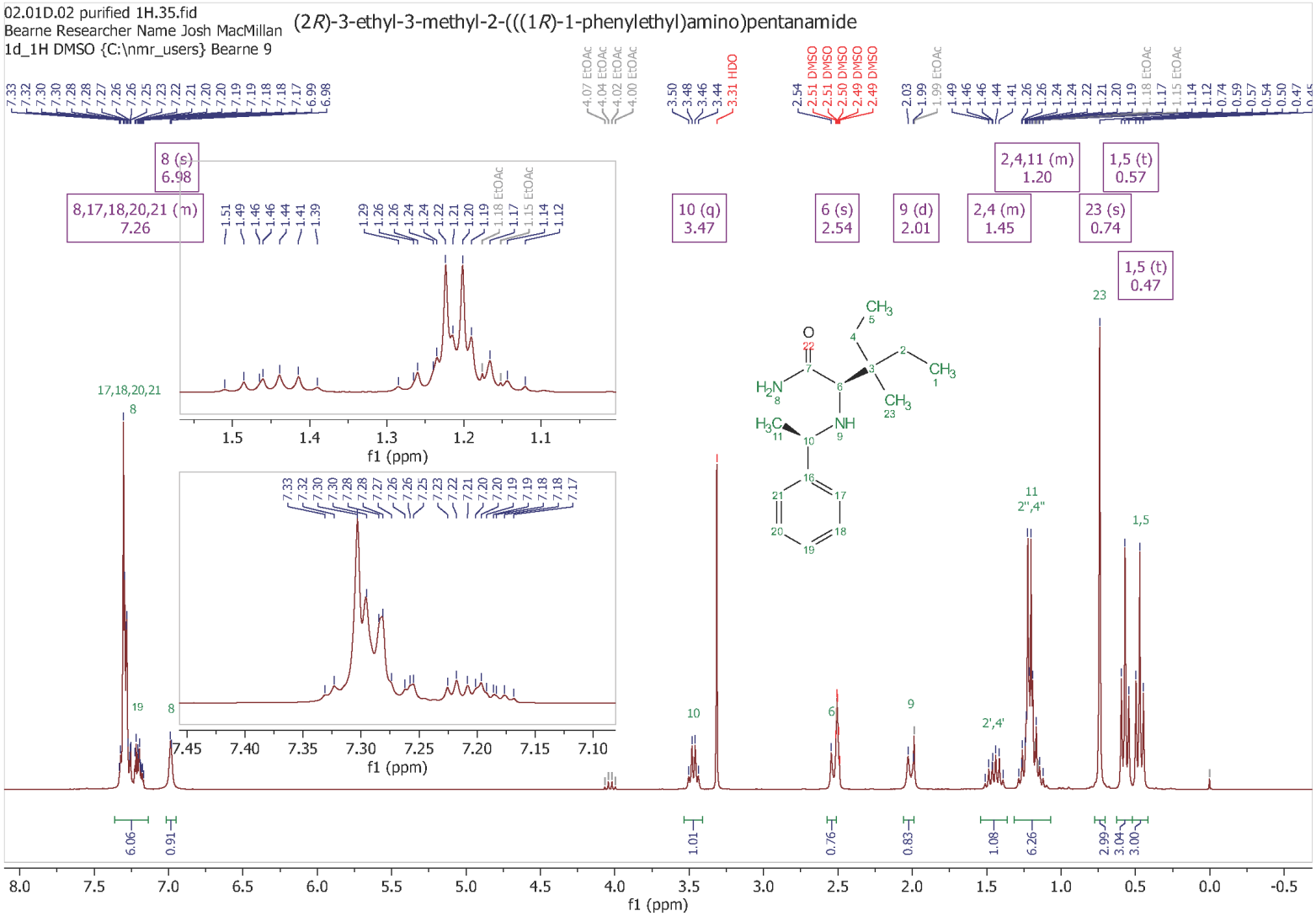

Figure S21

Figure S22. ^{13}C NMR spectrum of 3-ethyl-3-methyl-N^2-[(1*R*)-1-phenylethyl]-D-norvalinamide (**9b**)

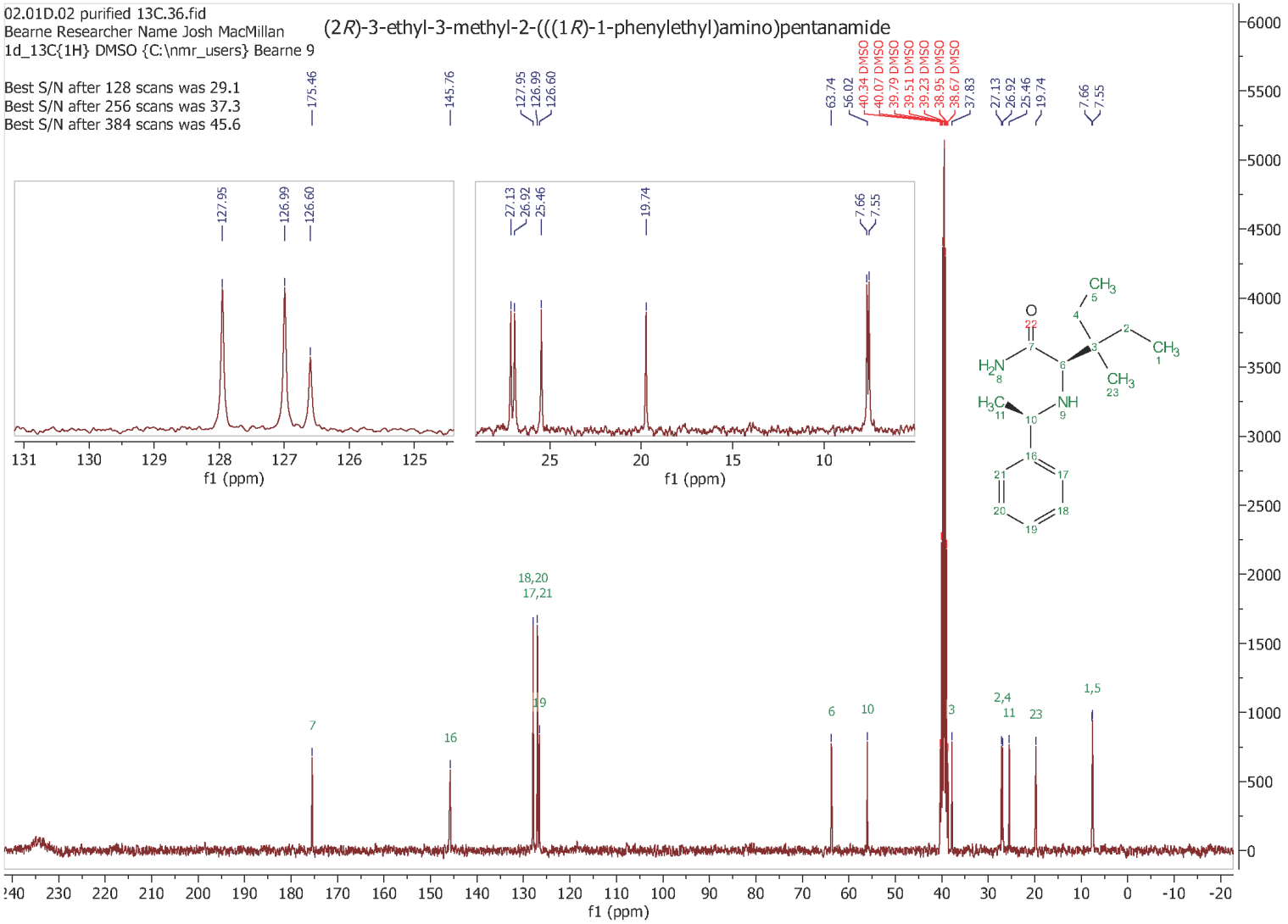

Figure S22

Figure S23. ^{1}H NMR spectrum of 3-ethyl-3-methyl-D-norvalinamide (**10b**)

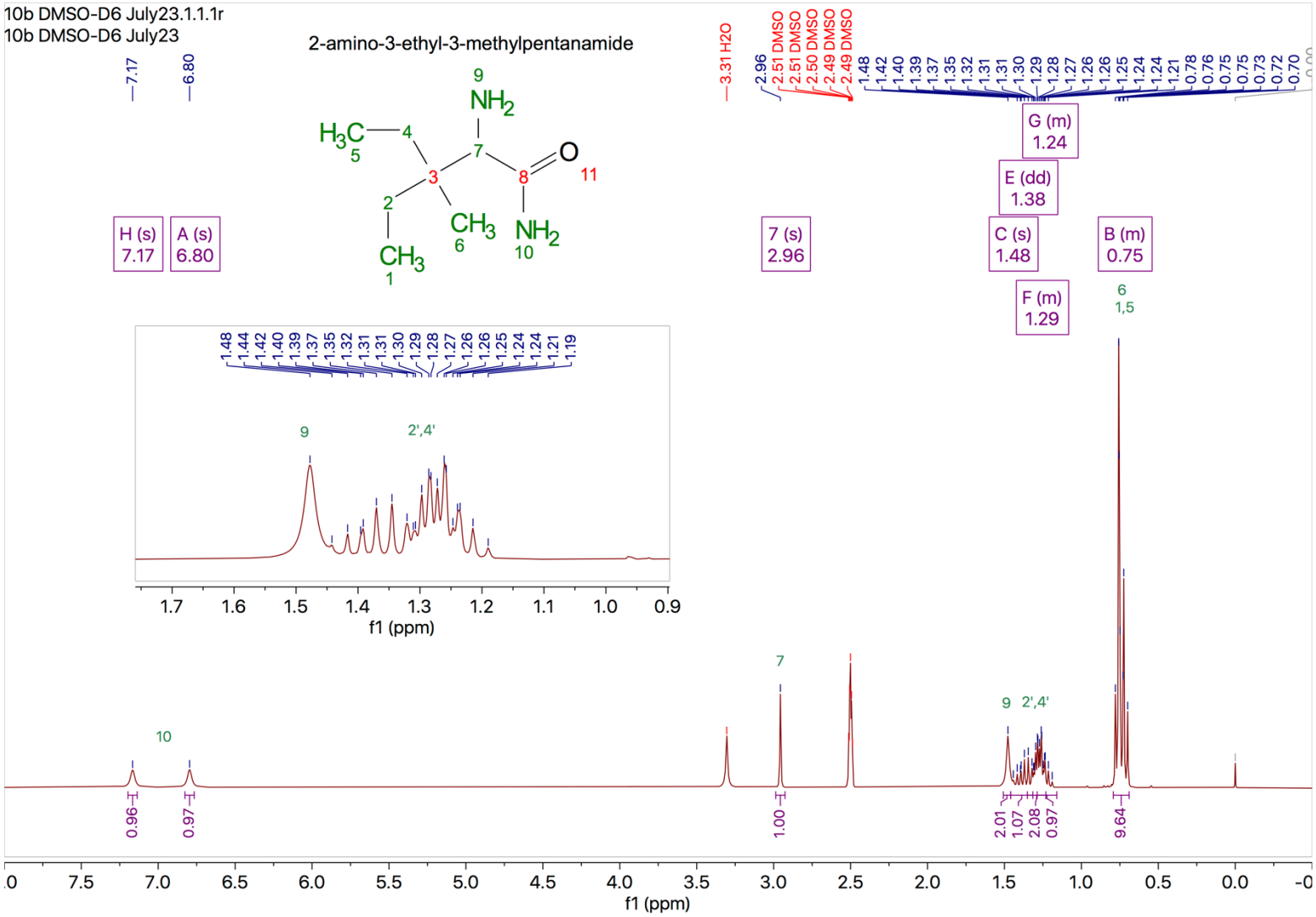

Figure S23

Figure S24. ^{13}C NMR spectrum of 3-ethyl-3-methyl-D-norvalinamide (**10b**)

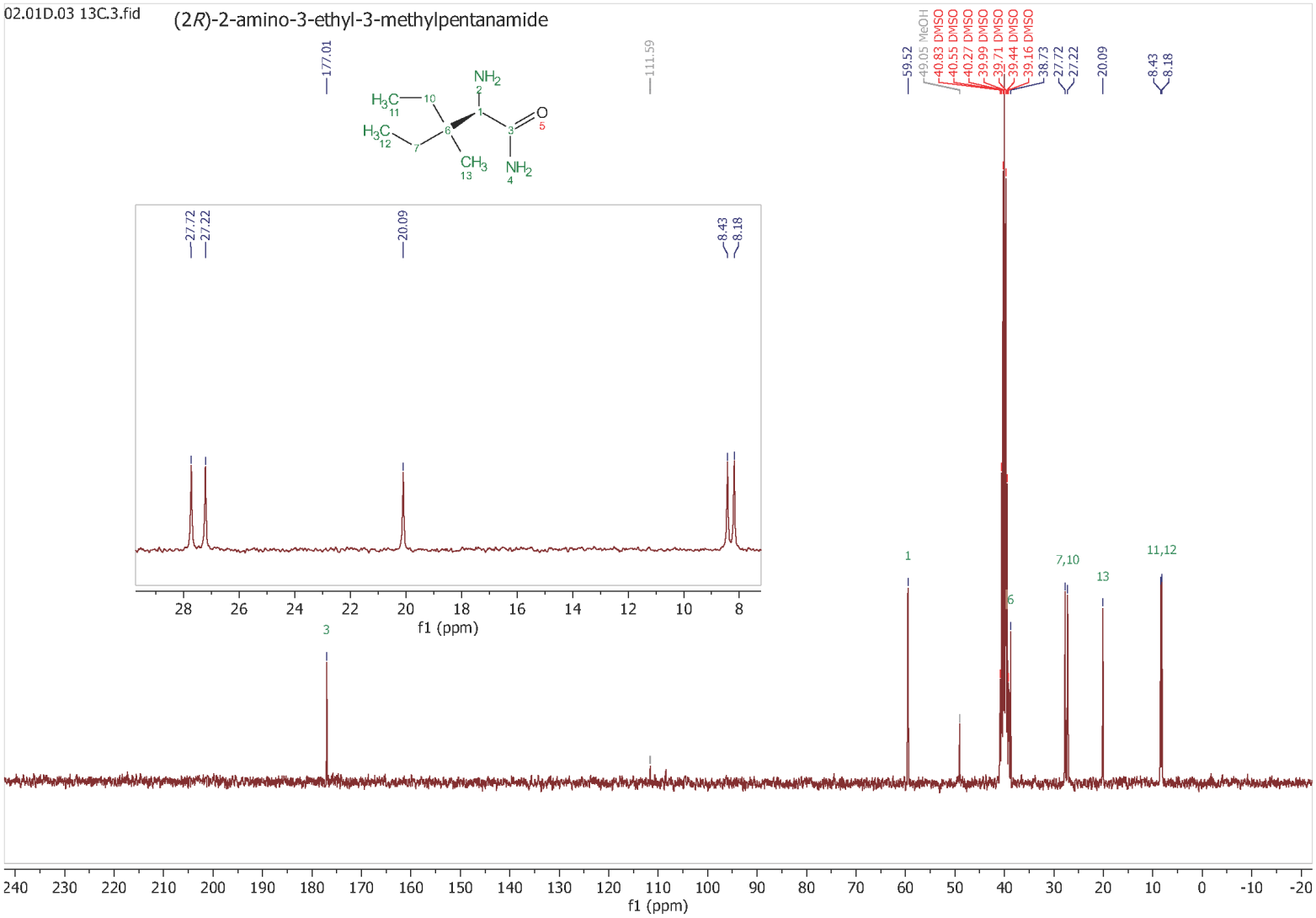

Figure S24

Figure S25. ^{1}H NMR spectrum of 3-ethyl-3-methyl-D-norvaline (**11b**)

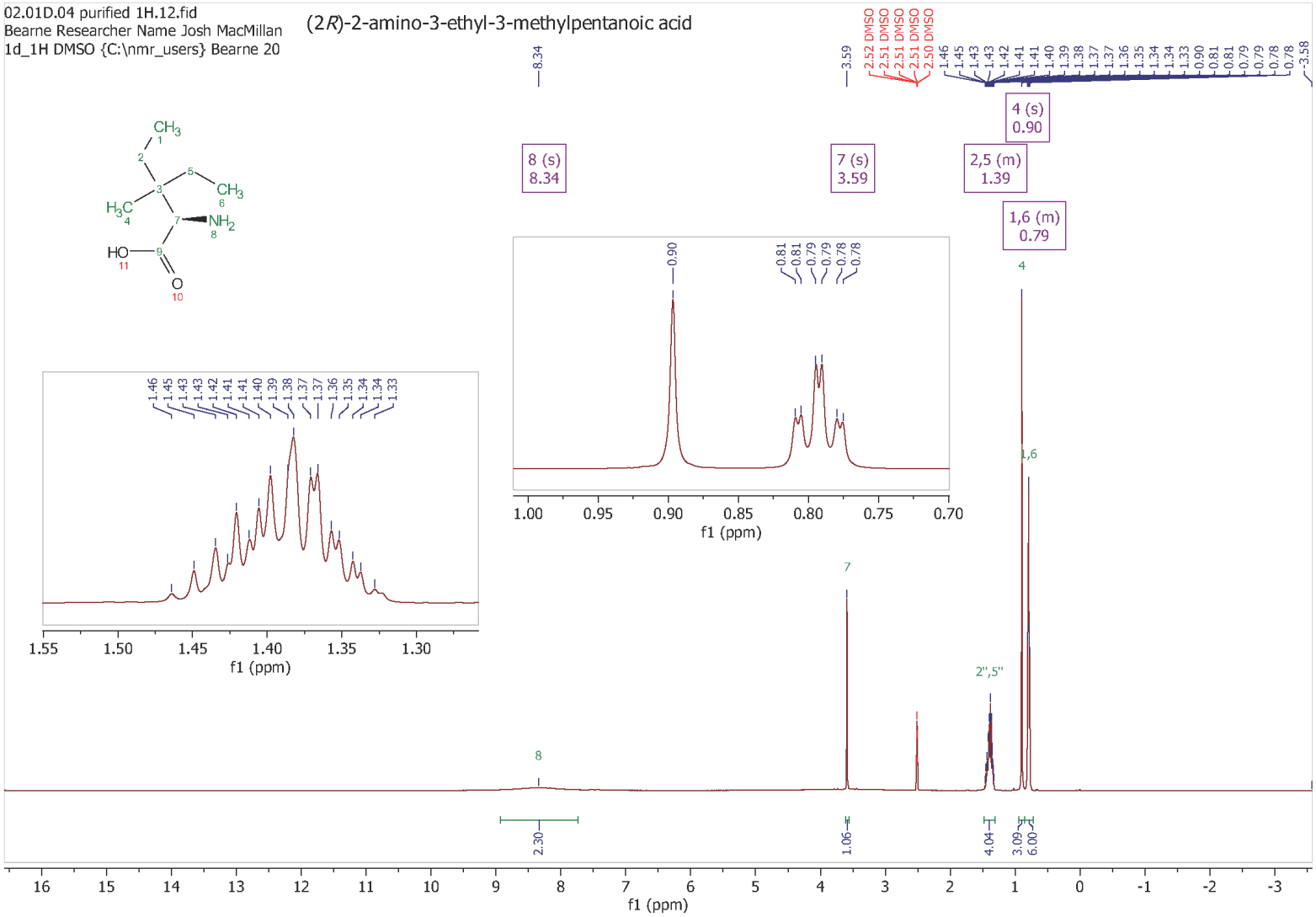

Figure S25

Figure S26. ^{13}C NMR spectrum of 3-ethyl-3-methyl-D-norvaline (**11b**)

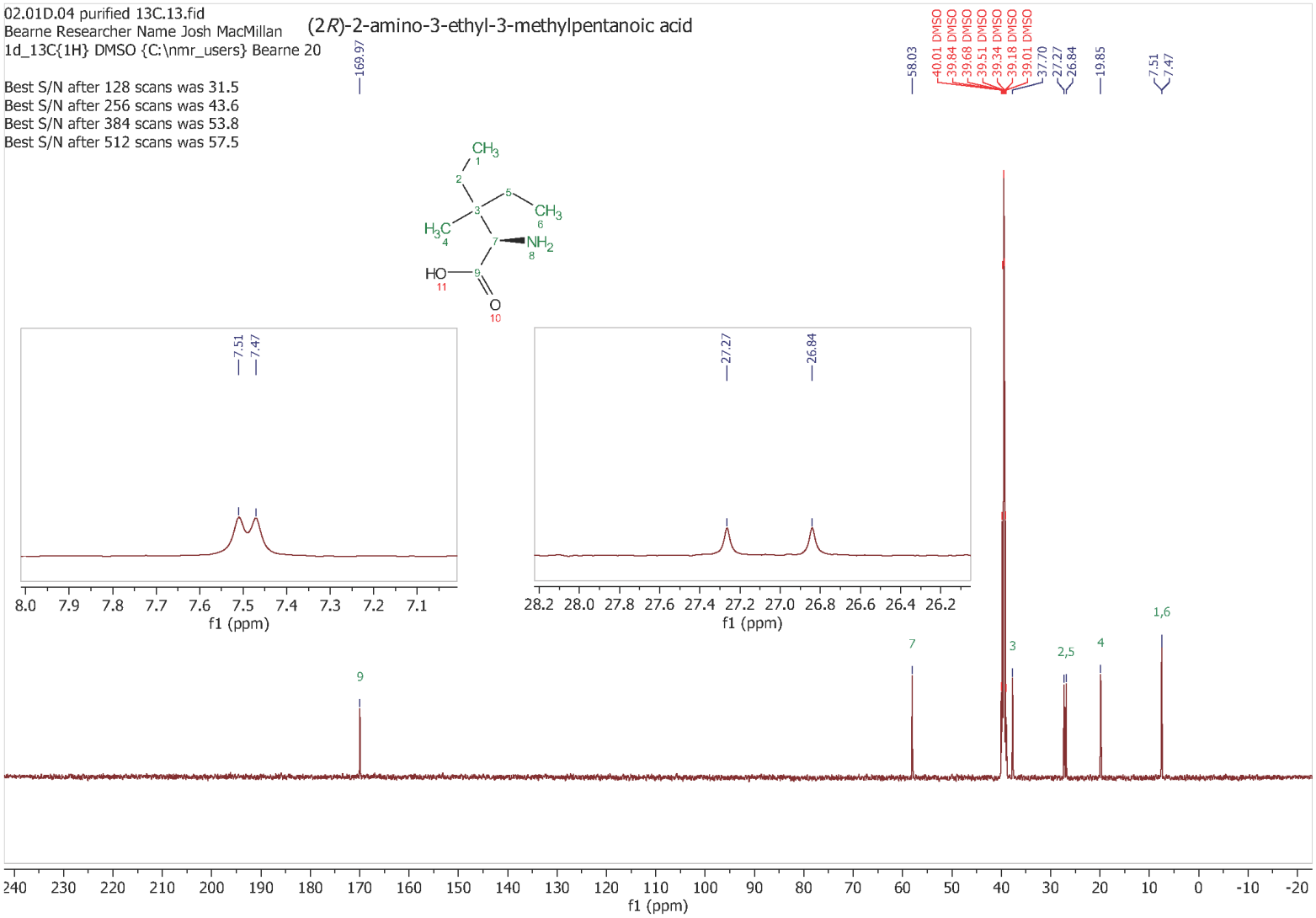

Figure S26

Figure S27. High resolution mass spectrum of 3-ethyl-L-norvaline (**6a**) – H^+ adduct

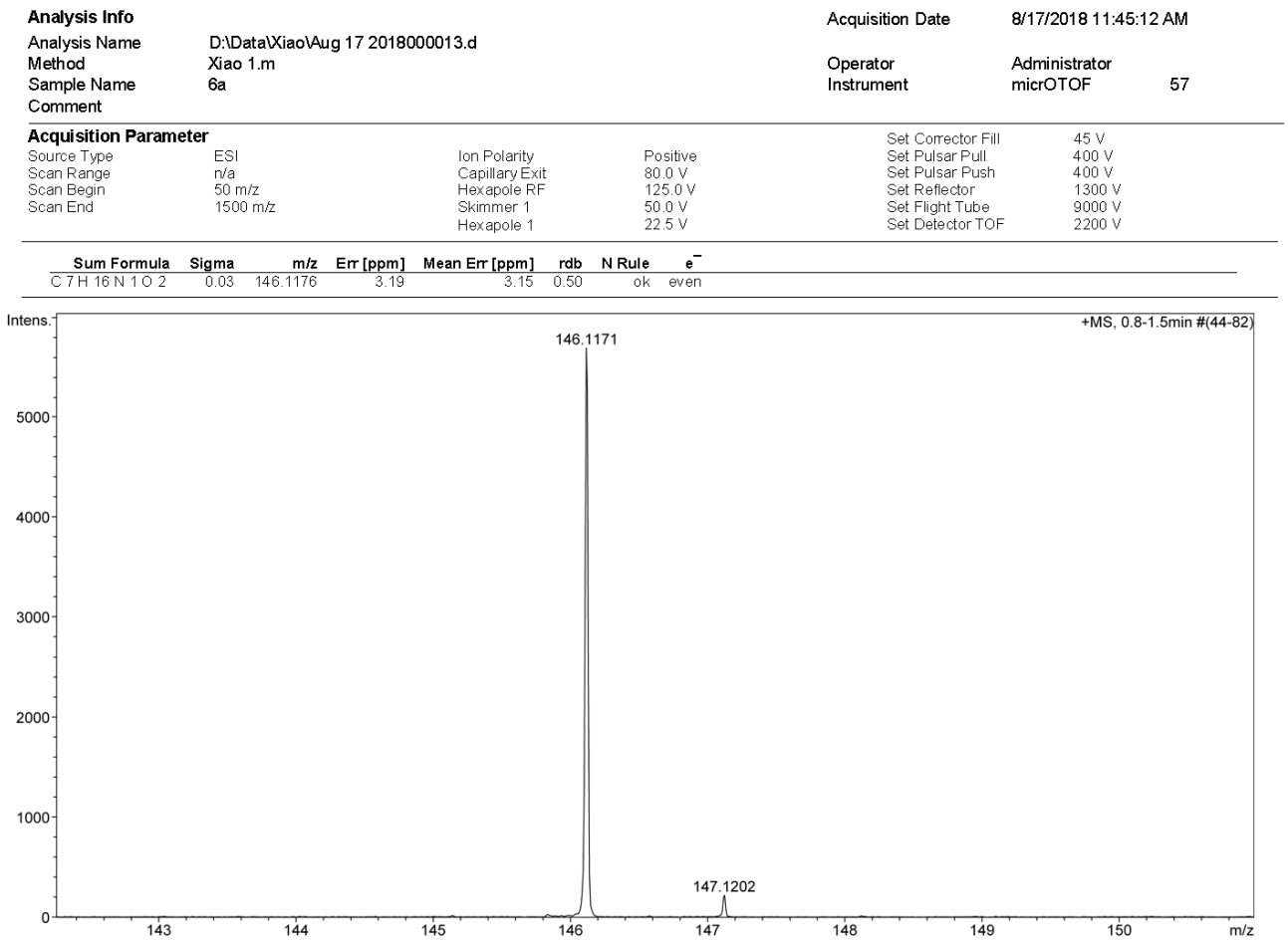

Figure S27

Figure S28. High resolution mass spectrum of 3-ethyl-L-norvaline (**6a**) – Na^+ adduct

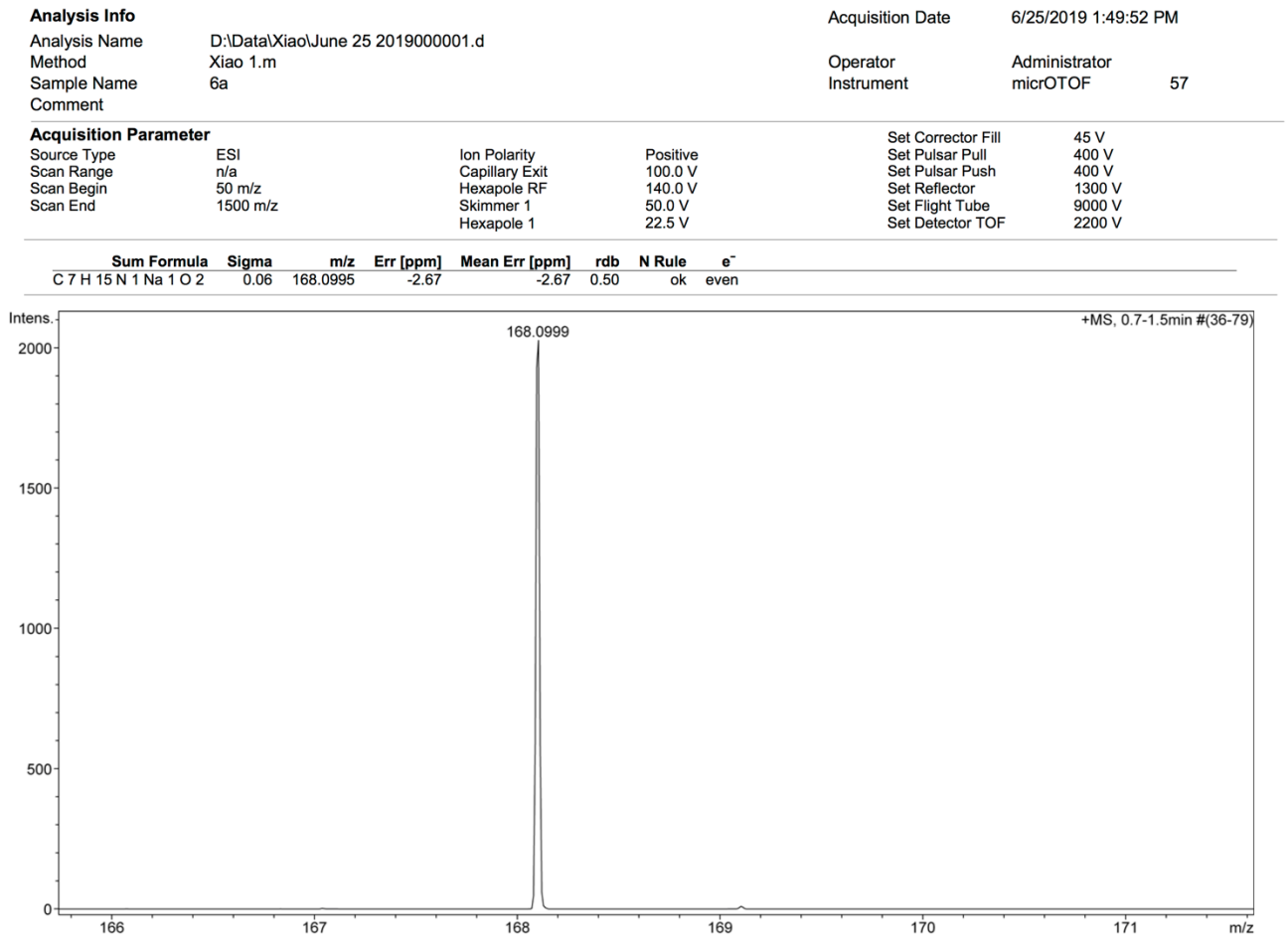

Figure S28

Figure S29. High resolution mass spectrum of (2*S*)-3-ethyl-3-methyl-2-{[(1*S*)-1-phenylethyl]amino}pentanenitrile (**2b**)

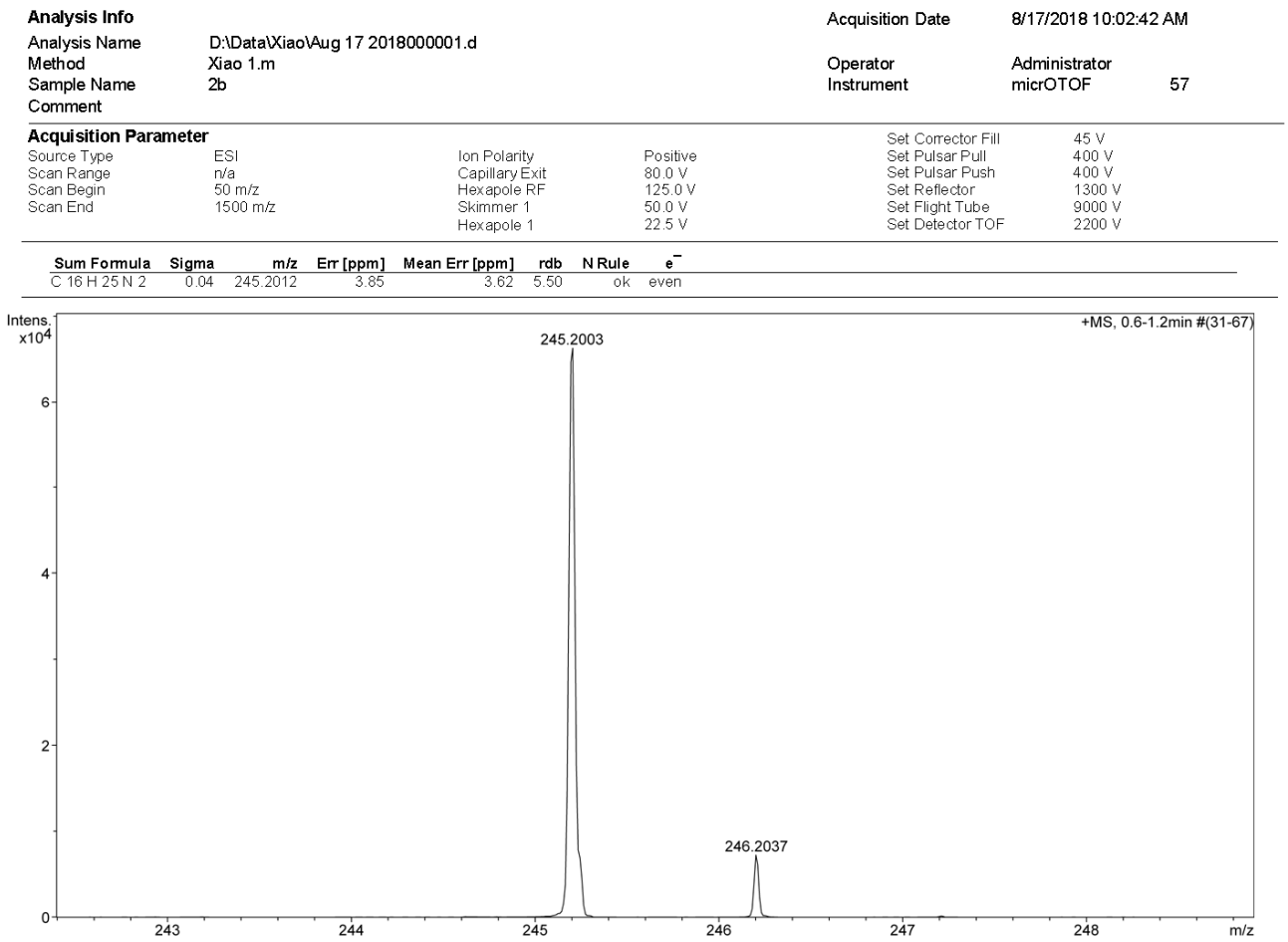

Figure S29

Figure S30. High resolution mass spectrum of 3-ethyl-3-methyl-N^2-[(1*S*)-1-phenylethyl]-L-norvalinamide (**4b**)

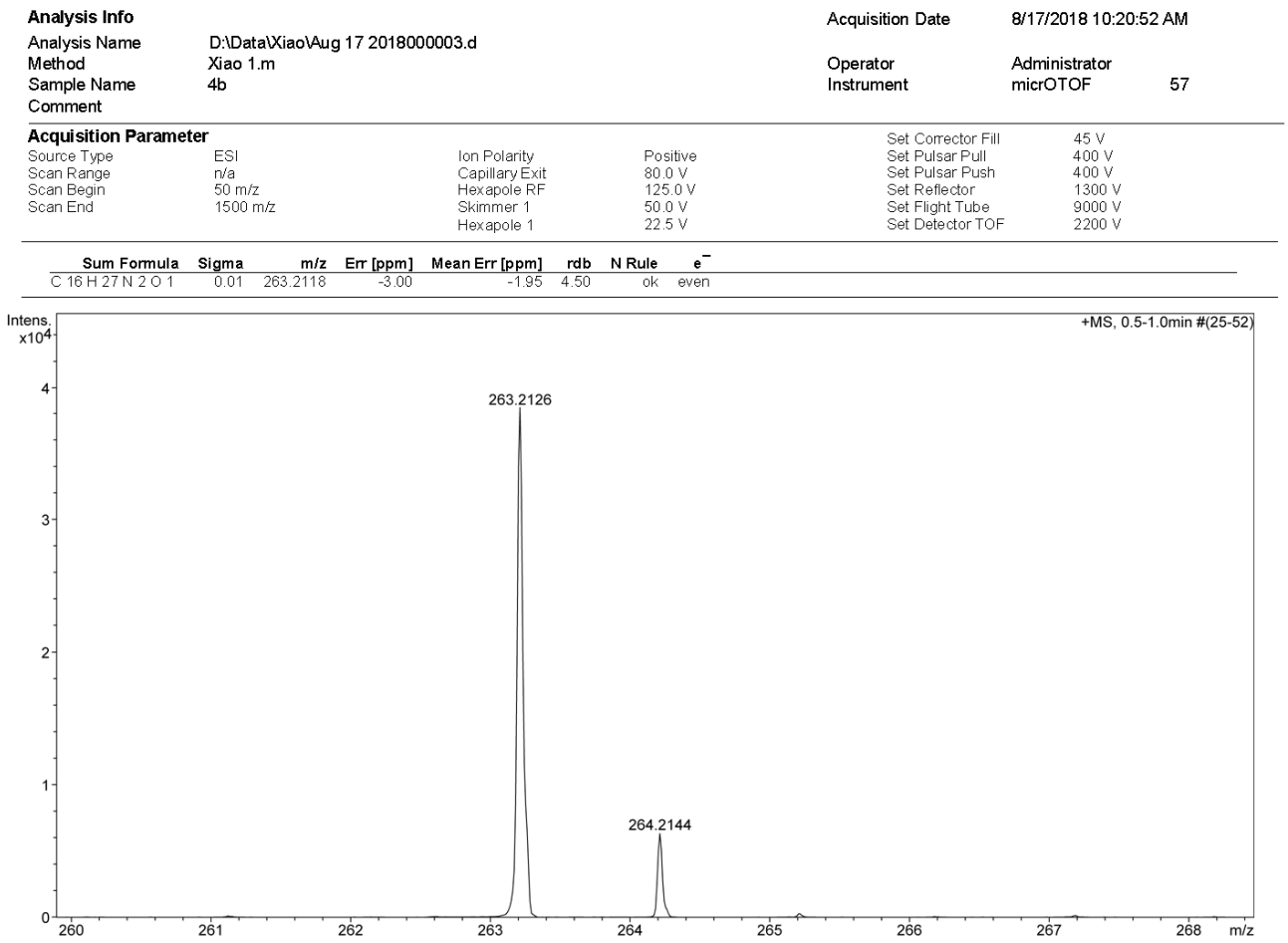

Figure S30

Figure S31. High resolution mass spectrum of 3-ethyl-3-methyl-L-norvalinamide (**5b**)

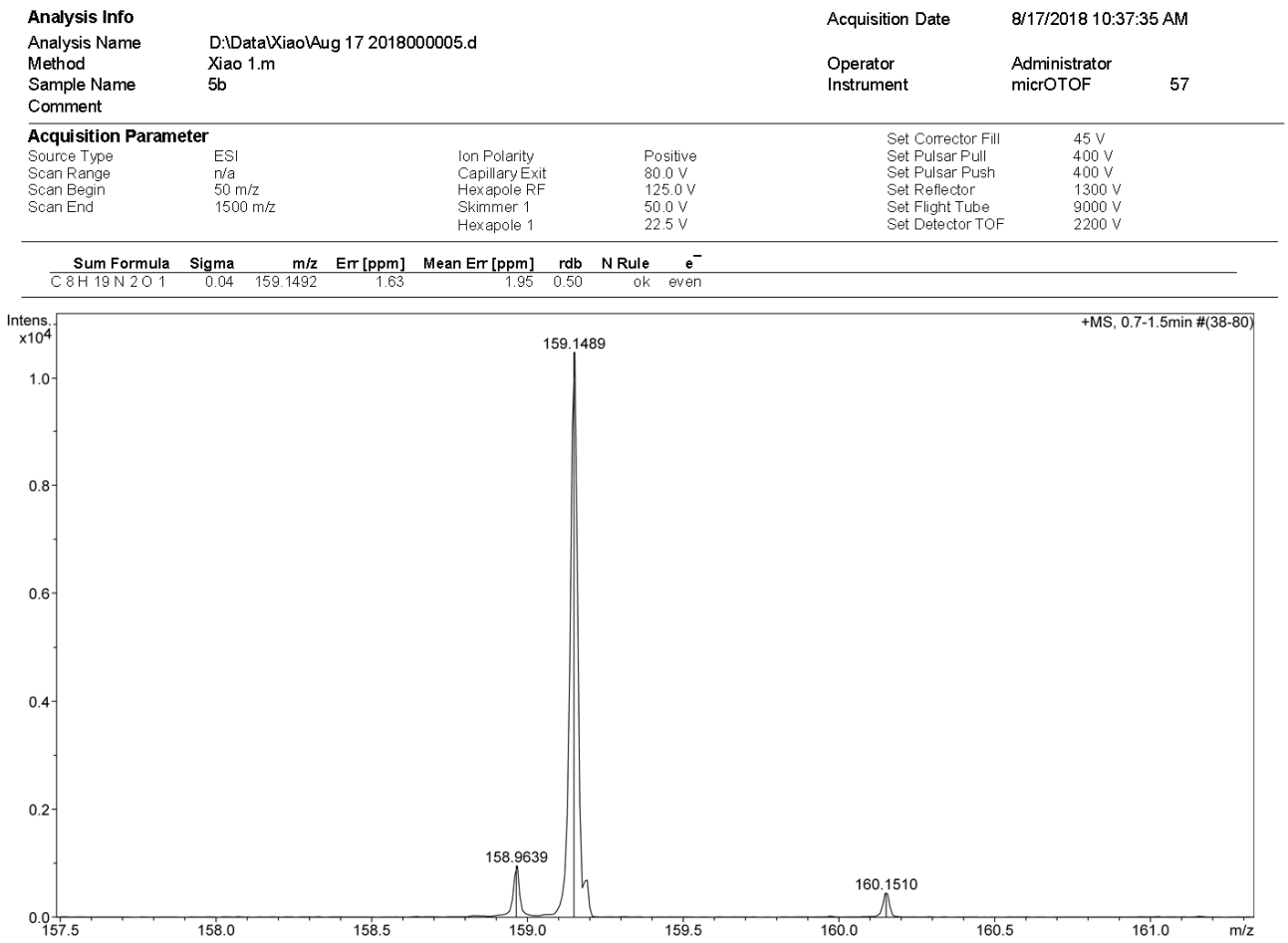

Figure S31

Figure S32. High resolution mass spectrum of 3-ethyl-3-methyl-L-norvaline (**6b**)

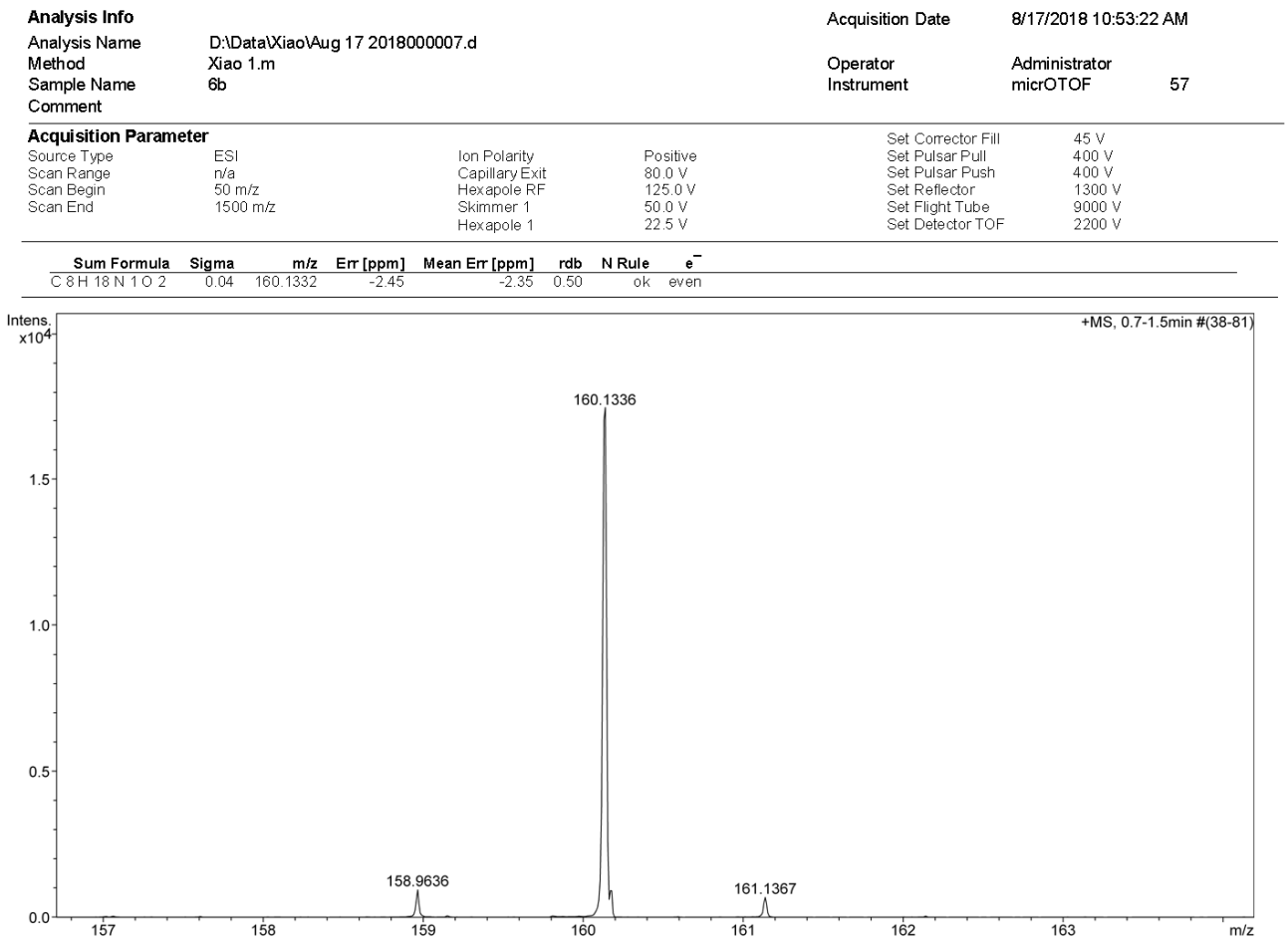

Figure S32

Figure S33. High resolution mass spectrum of (2*R*)-3-ethyl-2-{[1*R*)-1-phenylethyl]amino}pentanenitrile (**7a**)

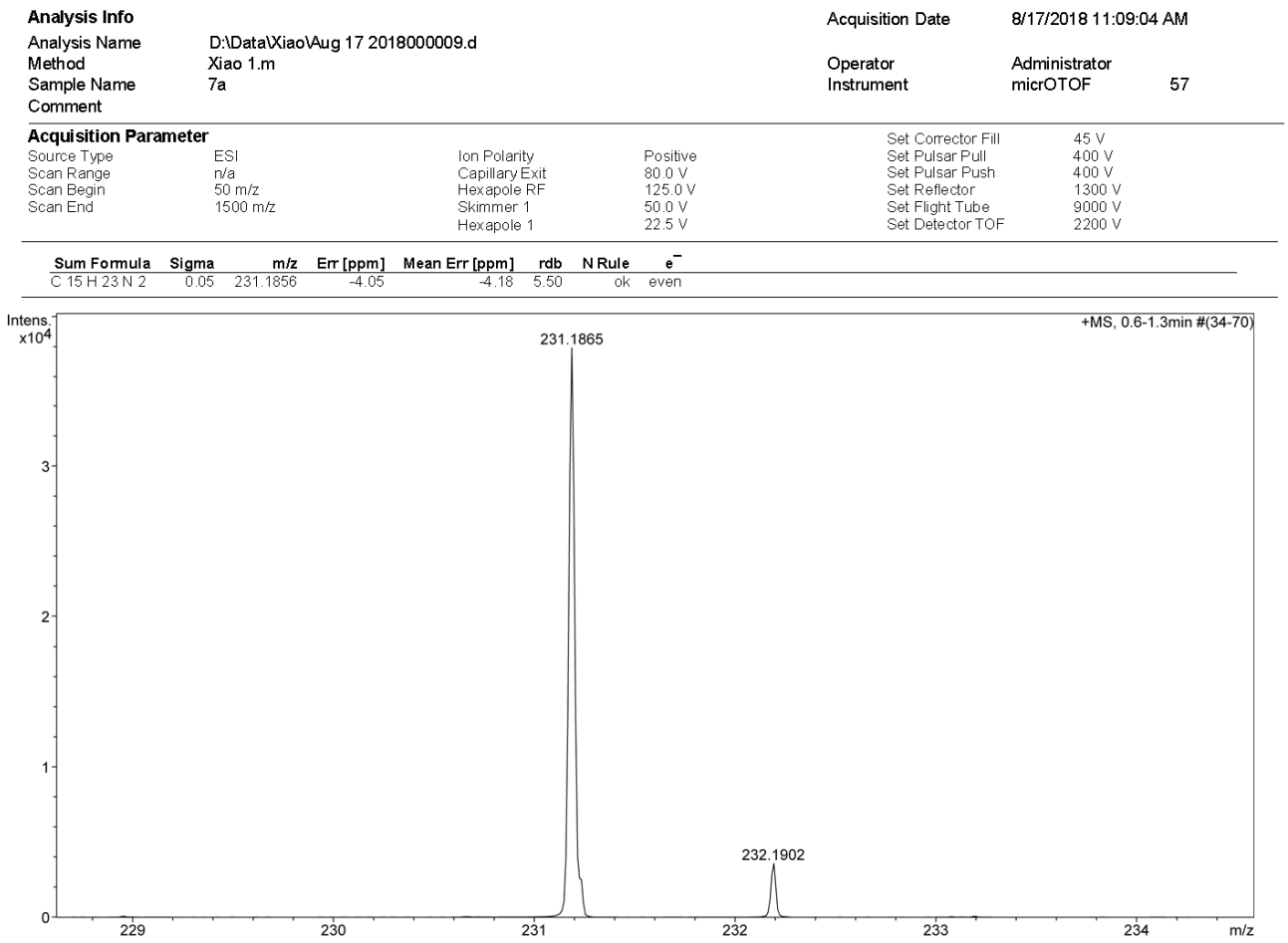

Figure S33

Figure S34. High resolution mass spectrum of 3-ethyl-N^2-[(1*R*)-1-phenylethyl]-D-norvalinamide (**9a**)

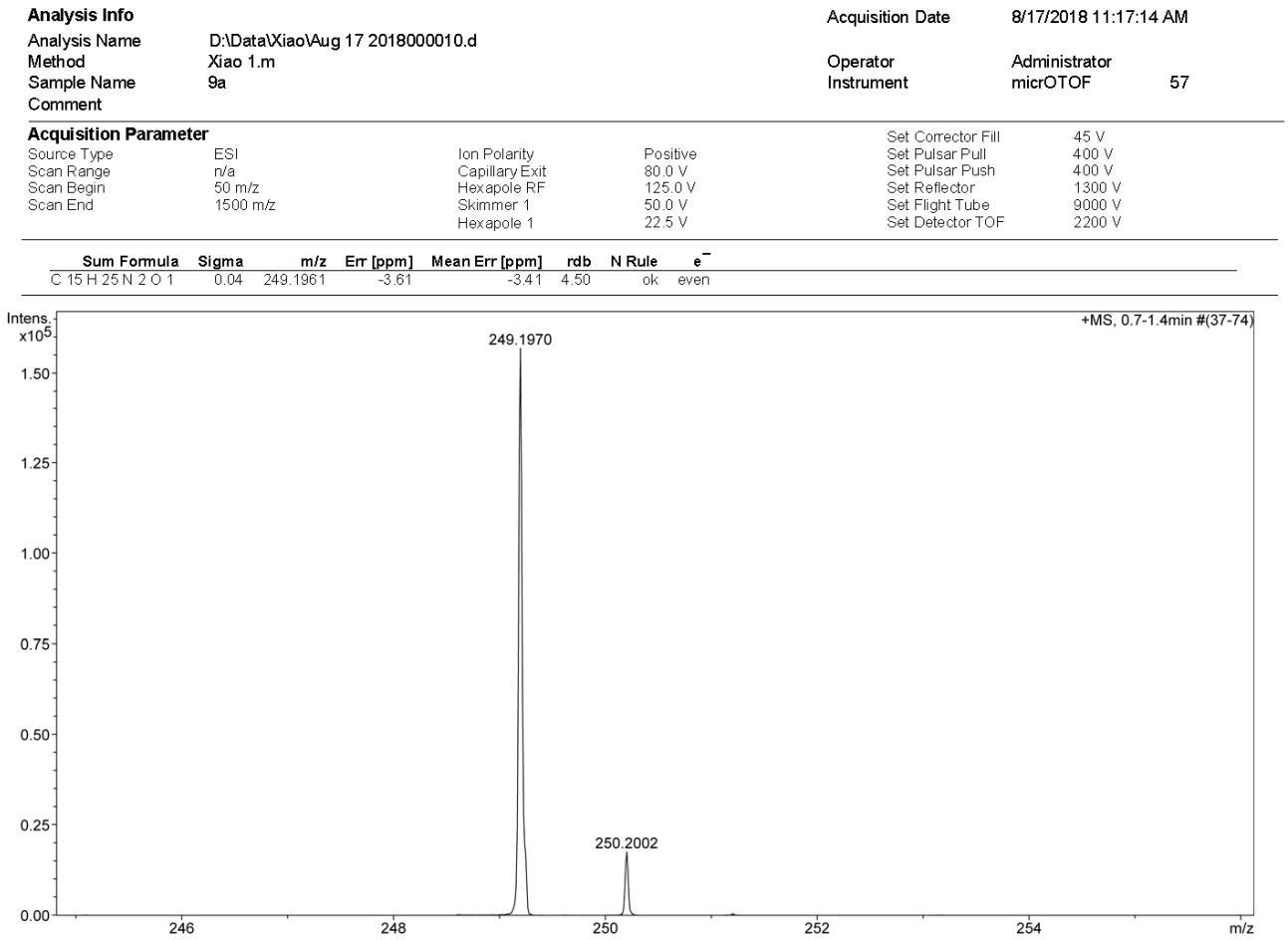

Figure S34

Figure S35. High resolution mass spectrum of 3-ethyl-D-norvalinamide (**10a**)

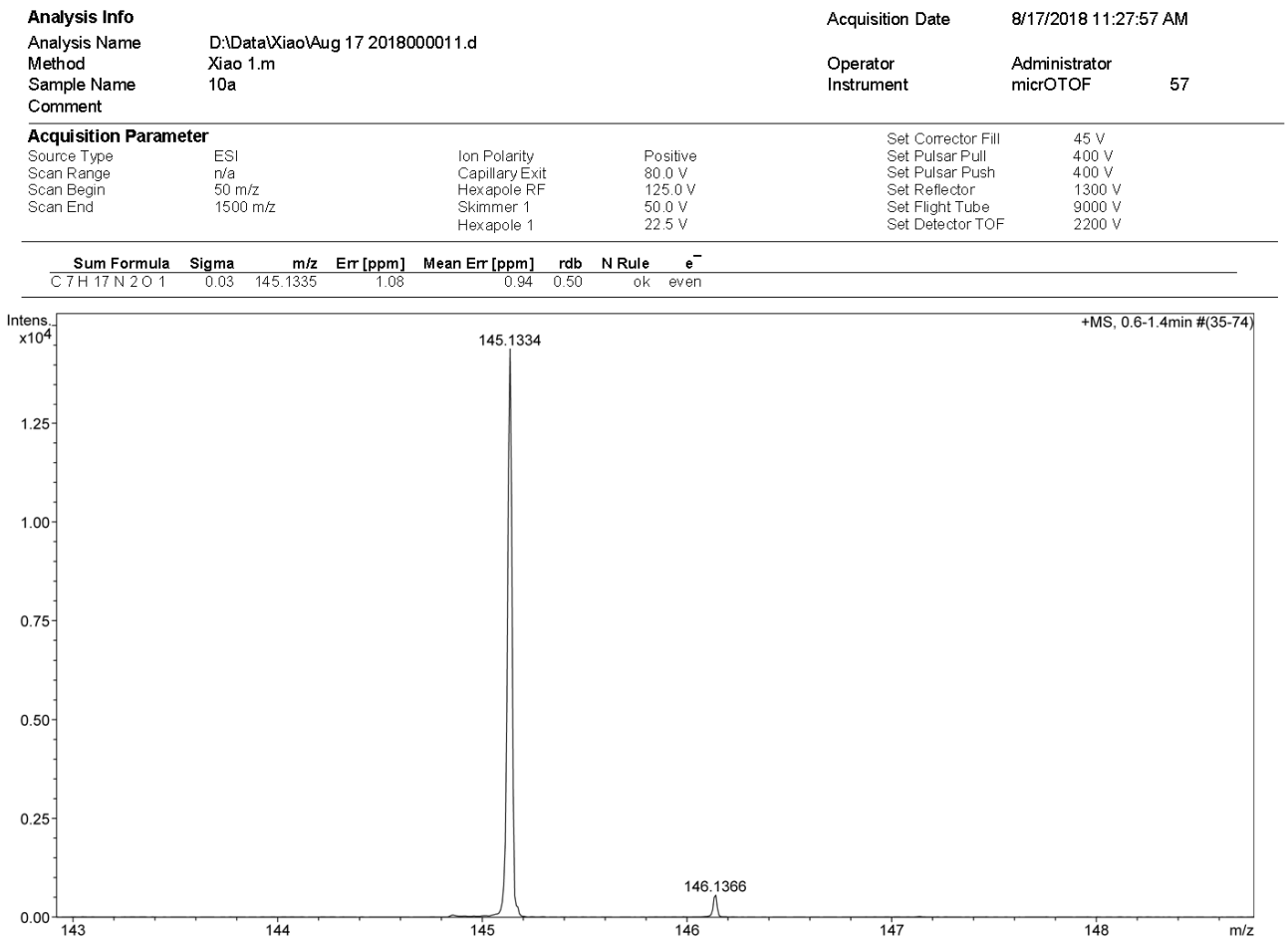

Figure S35

Figure S36. High resolution mass spectrum of 3-ethyl-D-norvaline (**11a**)

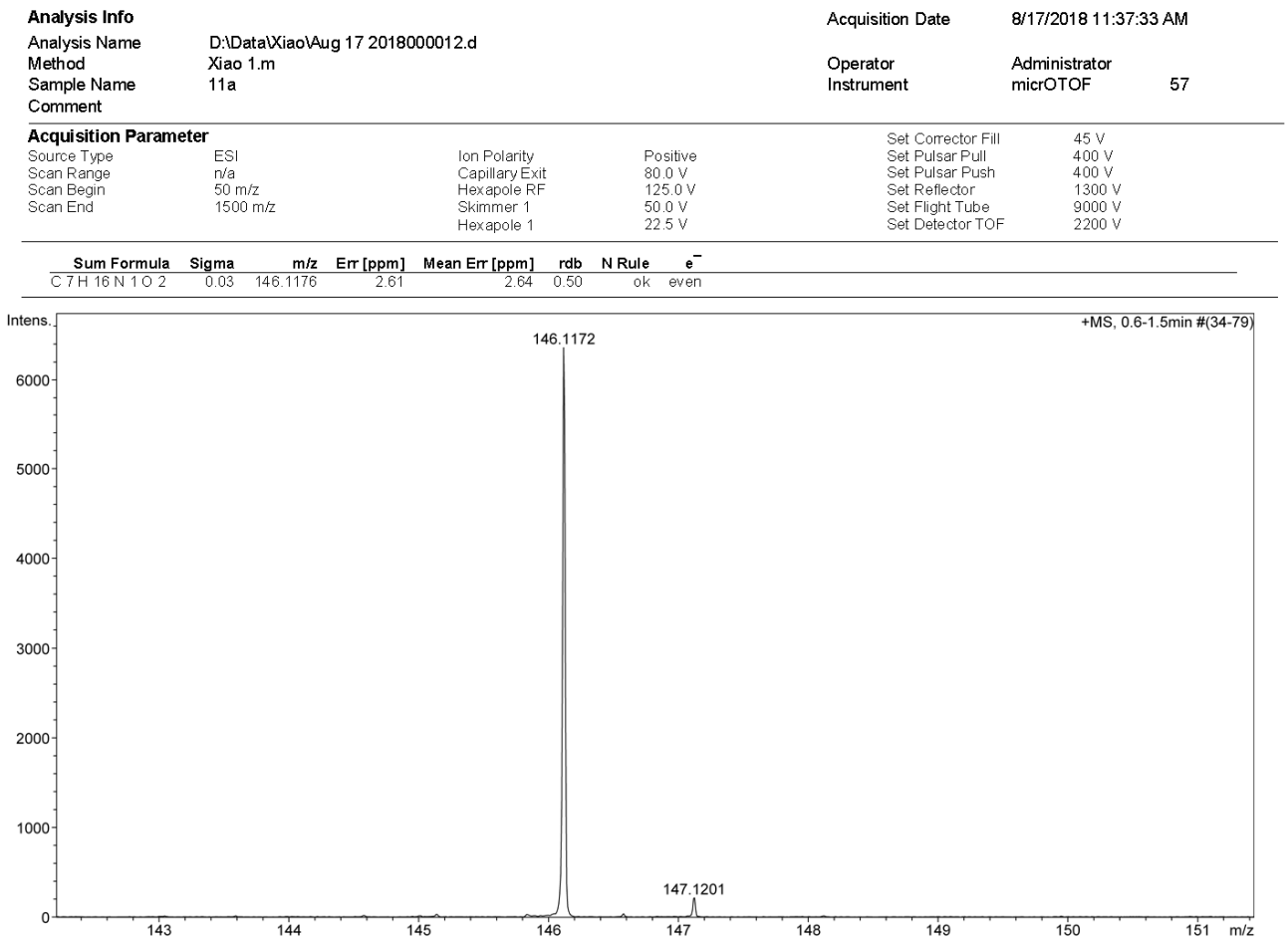

Figure S36

Figure S37. High resolution mass spectrum of (2*R*)-3-ethyl-3-methyl-2-{[(1*R*)-1-phenylethyl]amino}pentanenitrile (**7b**)

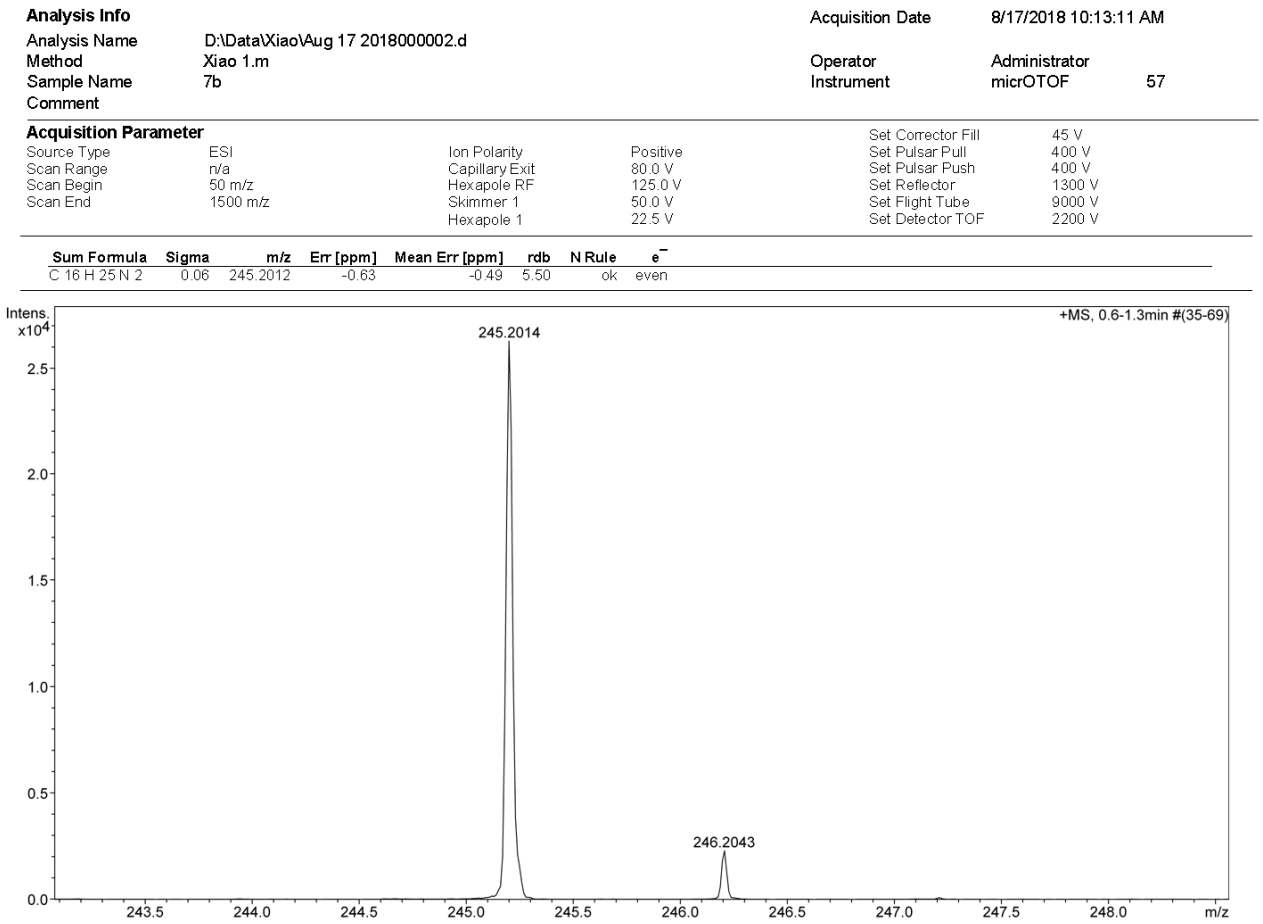

Figure S37

Figure S38. High resolution mass spectrum of 3-ethyl-3-methyl-N^2-[(1*R*)-1-phenylethyl]-D-norvalinamide (**9b**)

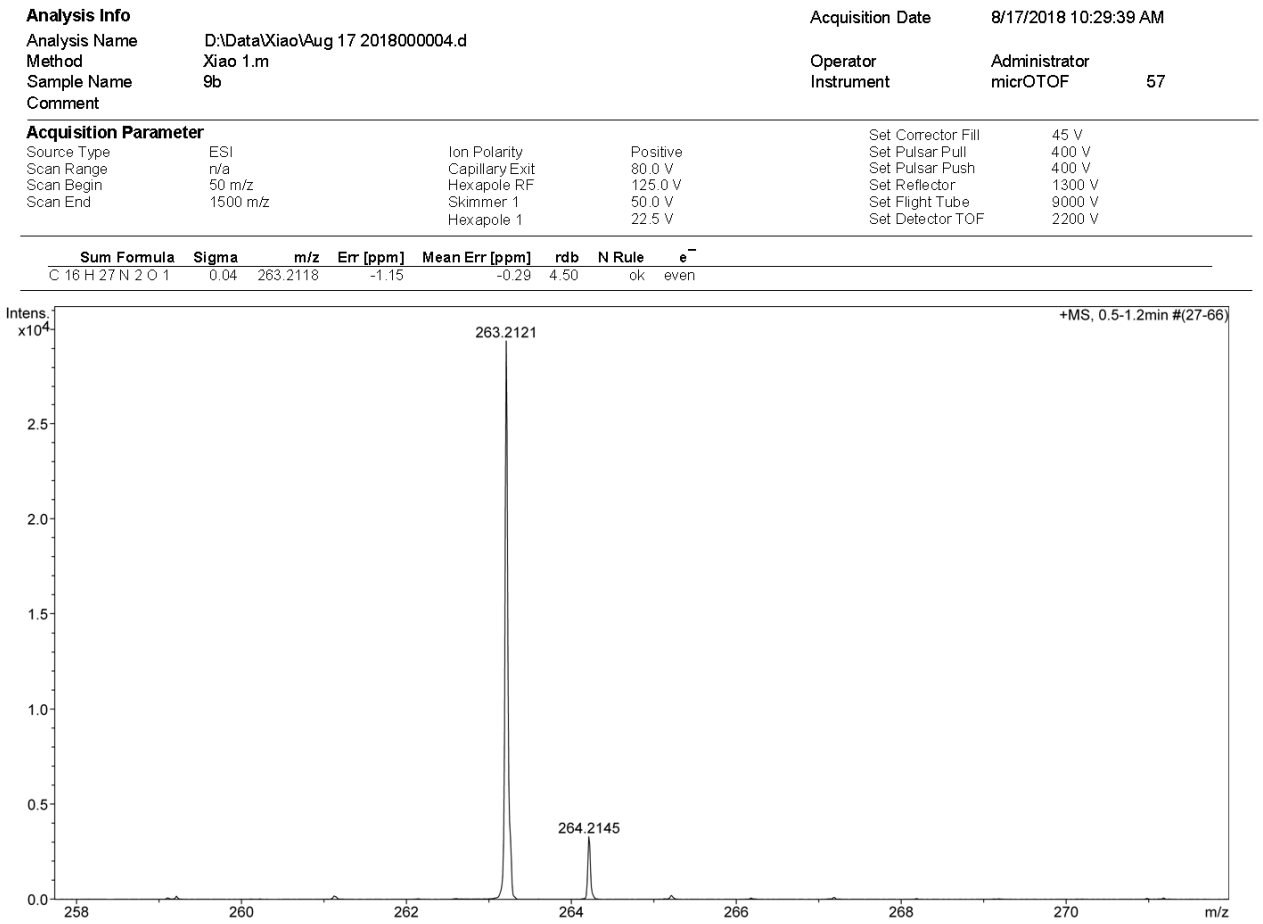

Figure S38

Figure S39. High resolution mass spectrum of 3-ethyl-3-methyl-D-norvalinamide (**10b**) – H+ adduct

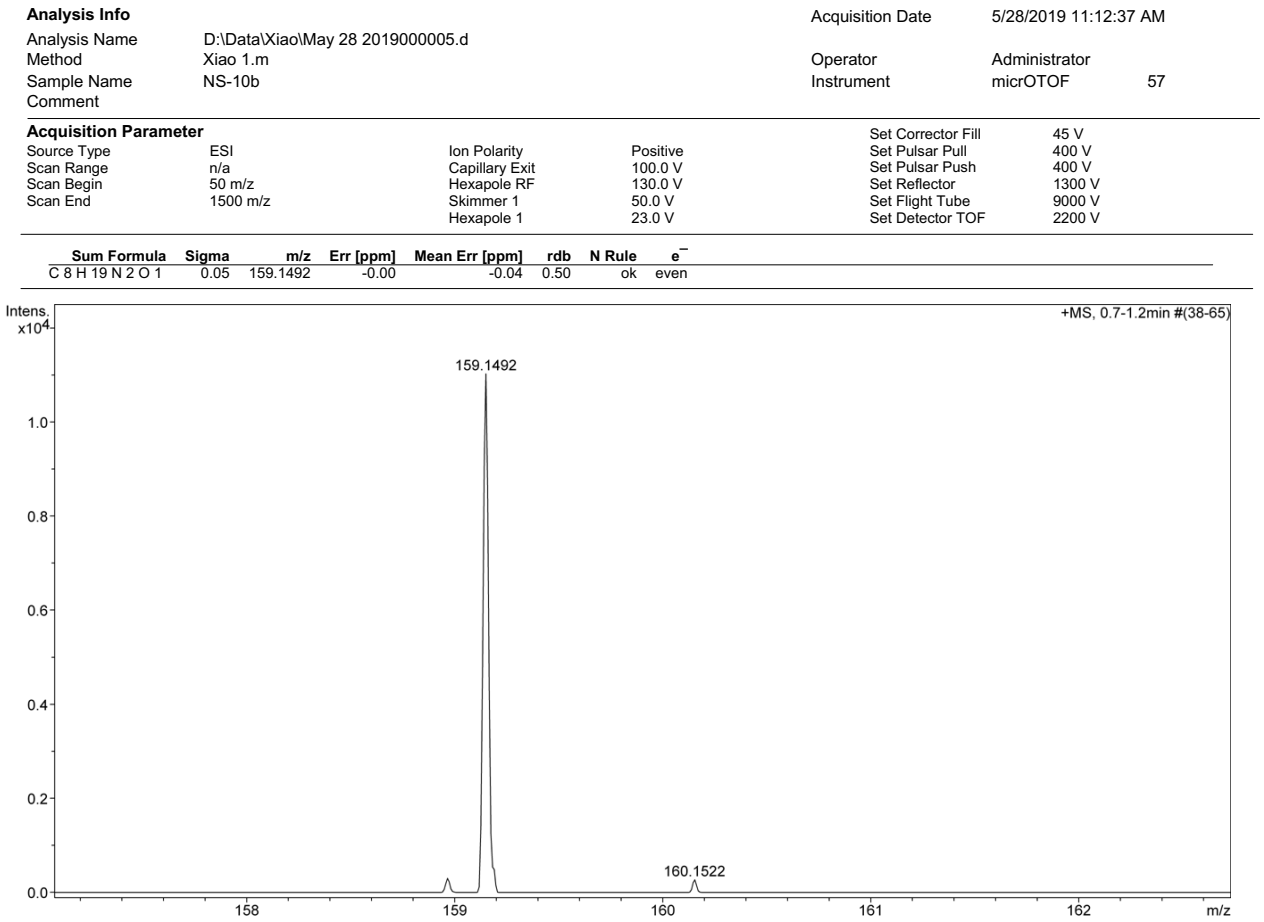

Figure S39

Figure S40. High resolution mass spectrum of 3-ethyl-3-methyl-D-norvalinamide (**10b**) – Na^+ adduct

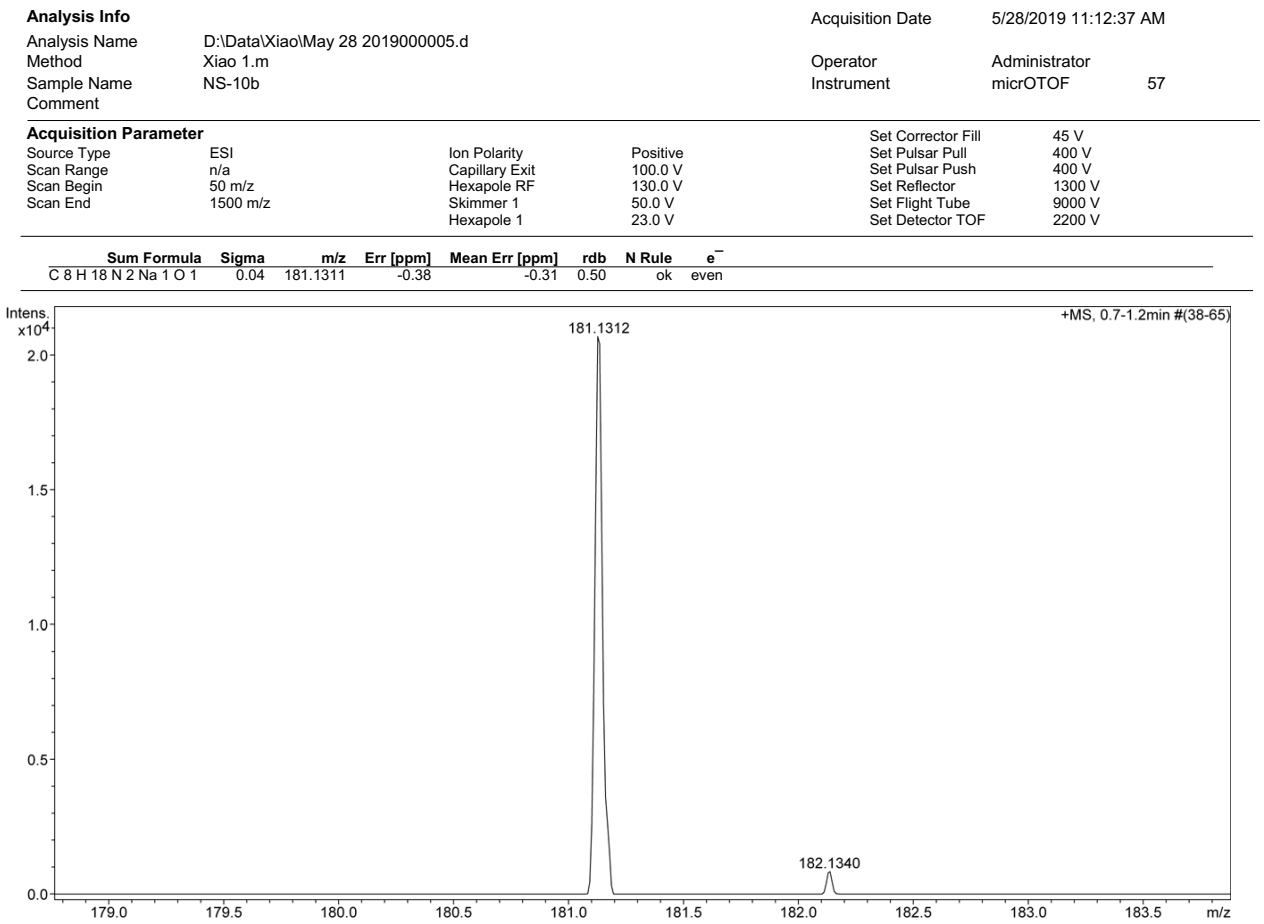

Figure S40

Figure S41. High resolution mass spectrum of 3-ethyl-3-methyl-D-norvaline (**11b**)

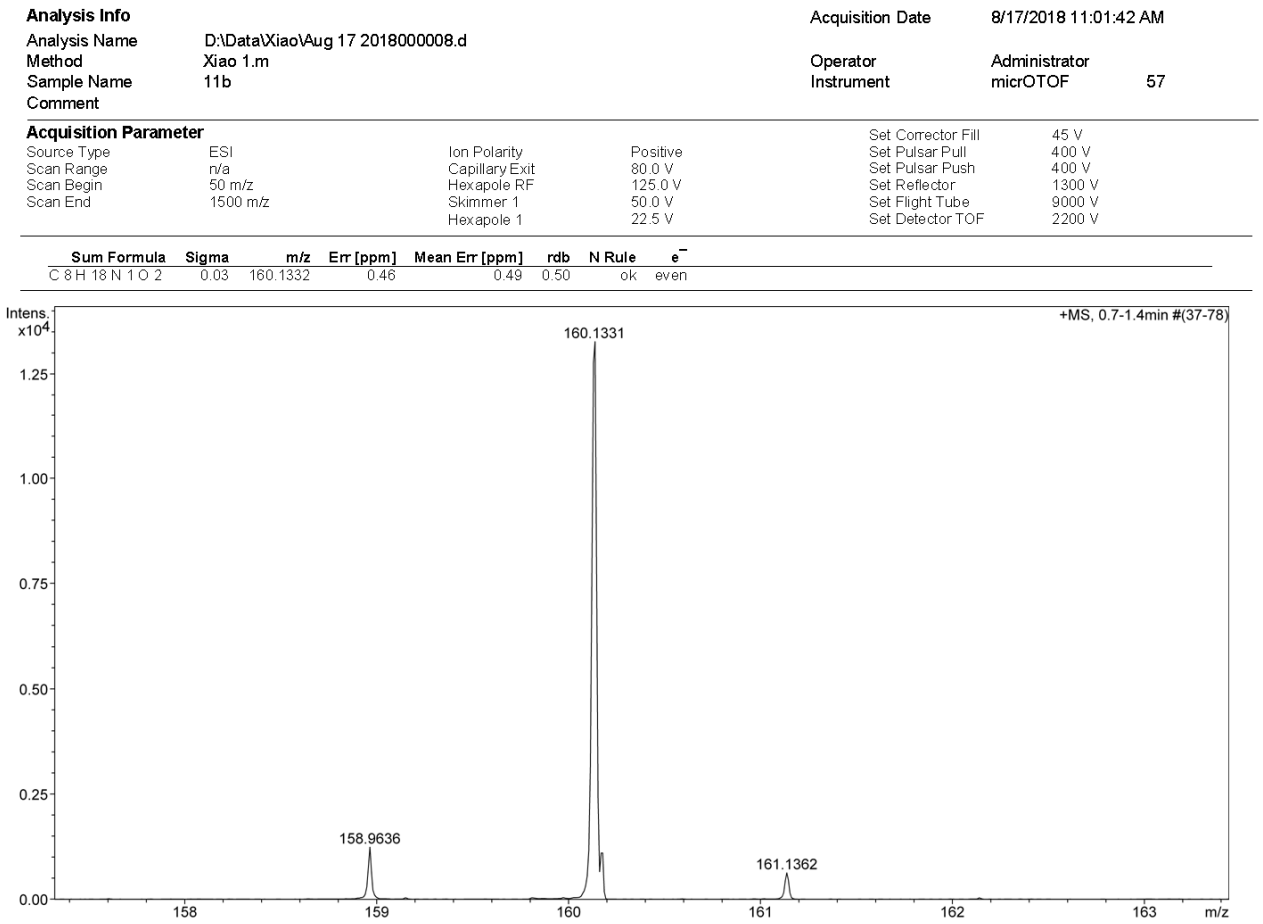

Figure S41

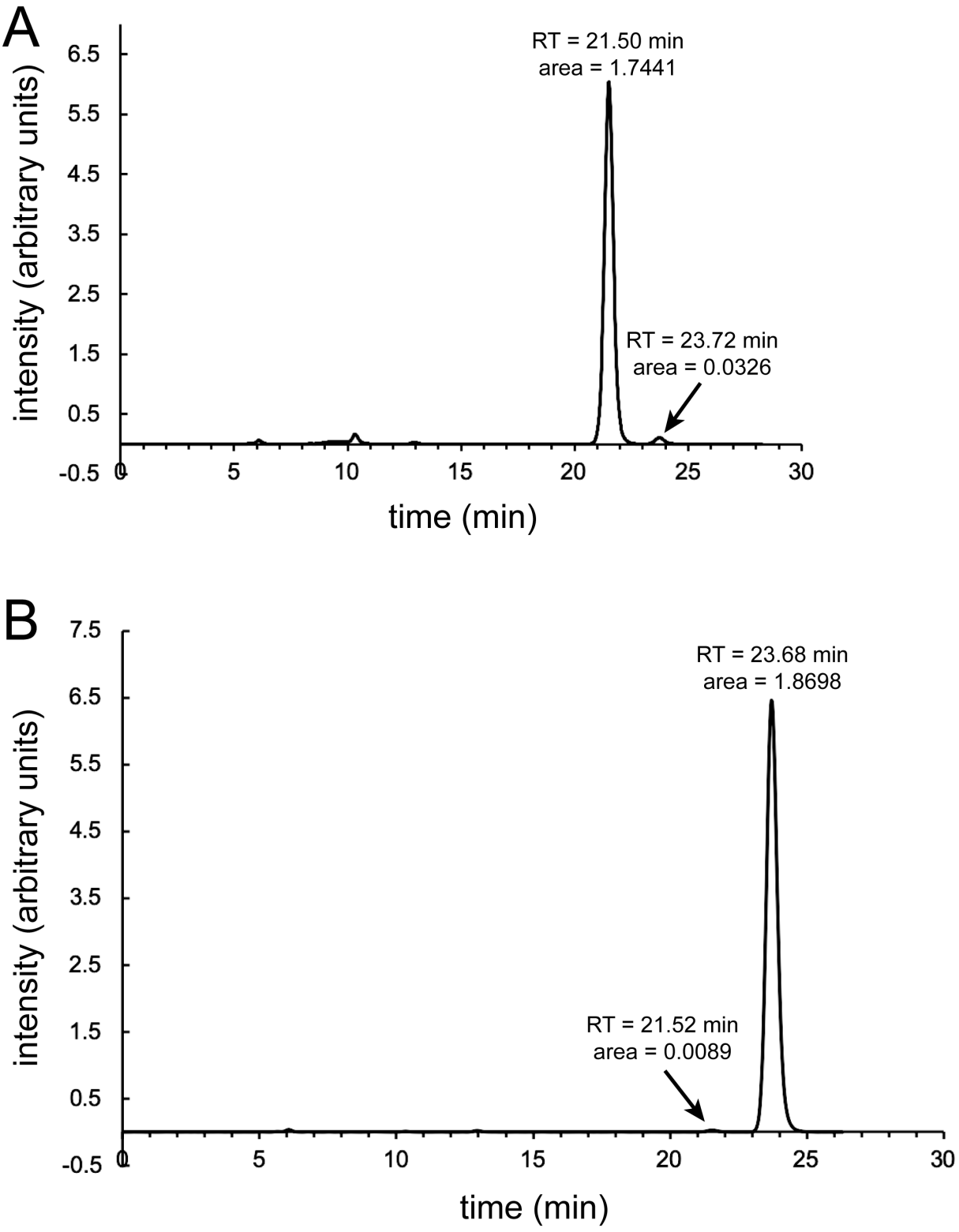
A
RT = 21.50 min
area = 1.7441
RT = 23.72 min
area = 0.0326
intensity (arbitrary units)
time (min)
B
RT = 23.68 min
area = 1.8698
RT = 21.52 min
area = 0.0089
intensity (arbitrary units)
time (min)

Figure S42

Figure S42. Representative HPLC chromatograms of derivatized **6a** (A) and **11a** (B). Compounds **6a** and **11a** were derivatized with *N*-acetyl-L-cysteine and OPA, and were separated on the reversed-phase column using isocratic elution with sodium acetate buffer (50 mM, pH 5.9):methanol (49:51). The %ee values for **6a** and **11a** are 96.3% and 99.1%, respectively. RT = retention time. See the Experimental section for additional details.

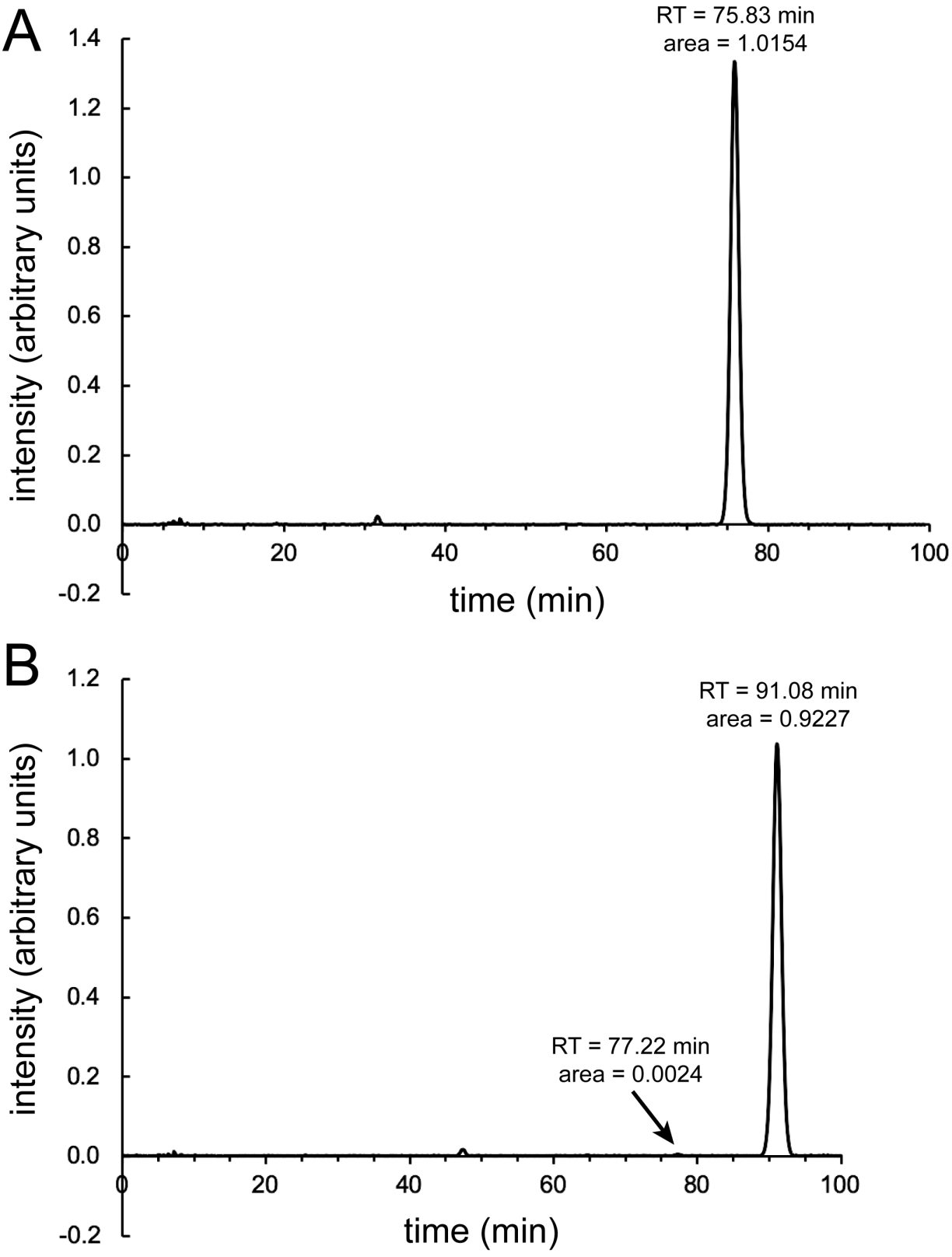
A
RT = 75.83 min
area = 1.0154
intensity (arbitrary units)
time (min)
B
RT = 91.08 min
area = 0.9227
RT = 77.22 min
area = 0.0024
intensity (arbitrary units)
time (min)

Figure S43

Figure S43. Representative HPLC chromatograms of derivatized **6b** (A) and **11b** (B). Compounds **6b** and **11b** were derivatized with *N*-acetylcysteine and OPA, and were separated on the reversed-phase column using isocratic elution with sodium acetate buffer (50 mM, pH 5.9):methanol (49:51). The %ee values for **6b** and **11b** are 100.0% and 98.0%, respectively. RT = retention time. See the Experimental section for additional details.

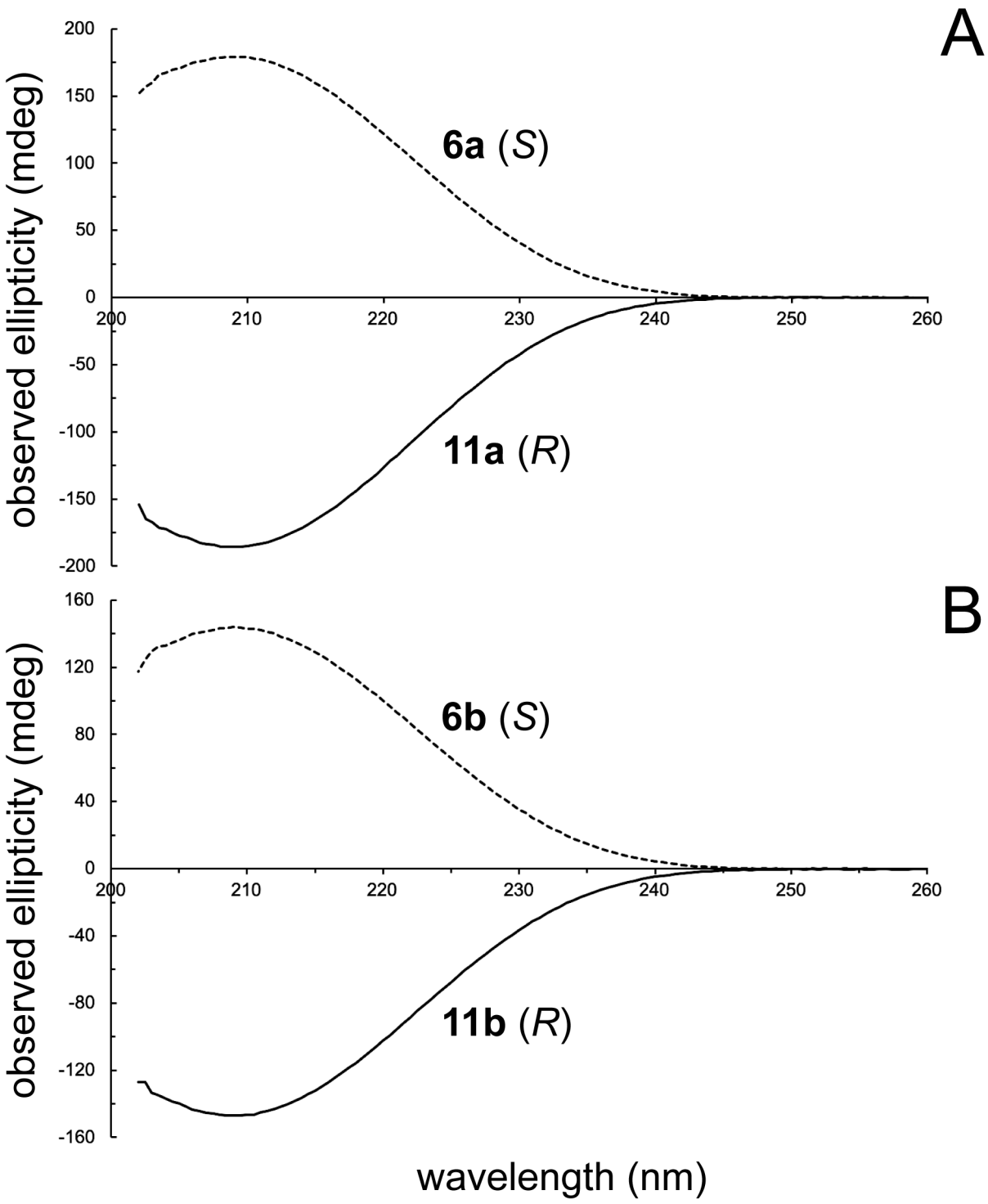

Figure S44. Representative circular dichroism spectra of the enantiomers of **6** and **11**. Spectra are shown for **6a** (---) and **11a** (—) in panel A, and for **6b** (---) and **11b** (—) in panel B. See the Experimental section for additional details.

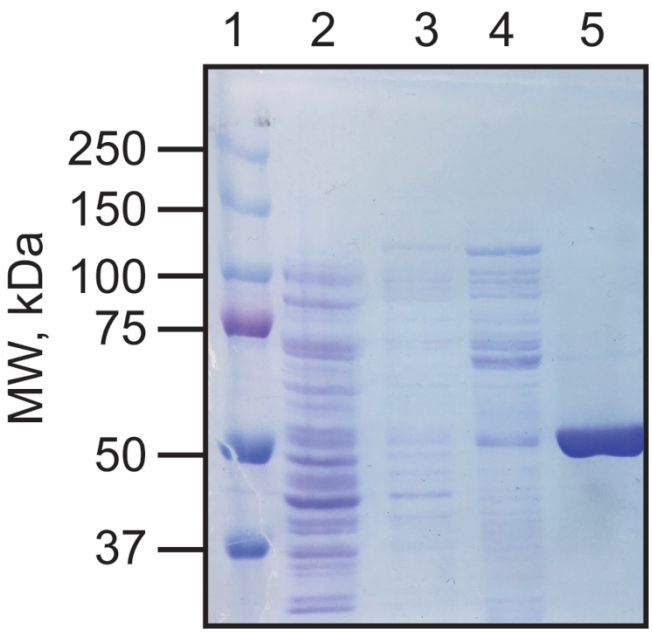

Figure S45. SDS-PAGE gel (8%) showing the purification of *Lb*IleE. Lane 1, molecular weight marker; lane 2, crude cell lysate; lane 3, binding buffer eluant; lane 4, wash buffer eluant; and lane 5, strip buffer eluant (purified *Lb*IleE post-dialysis). The calculated MW of the His_6-tagged *Lb*IleE fusion protein, based on the amino acid sequence, is 53 487 Da.

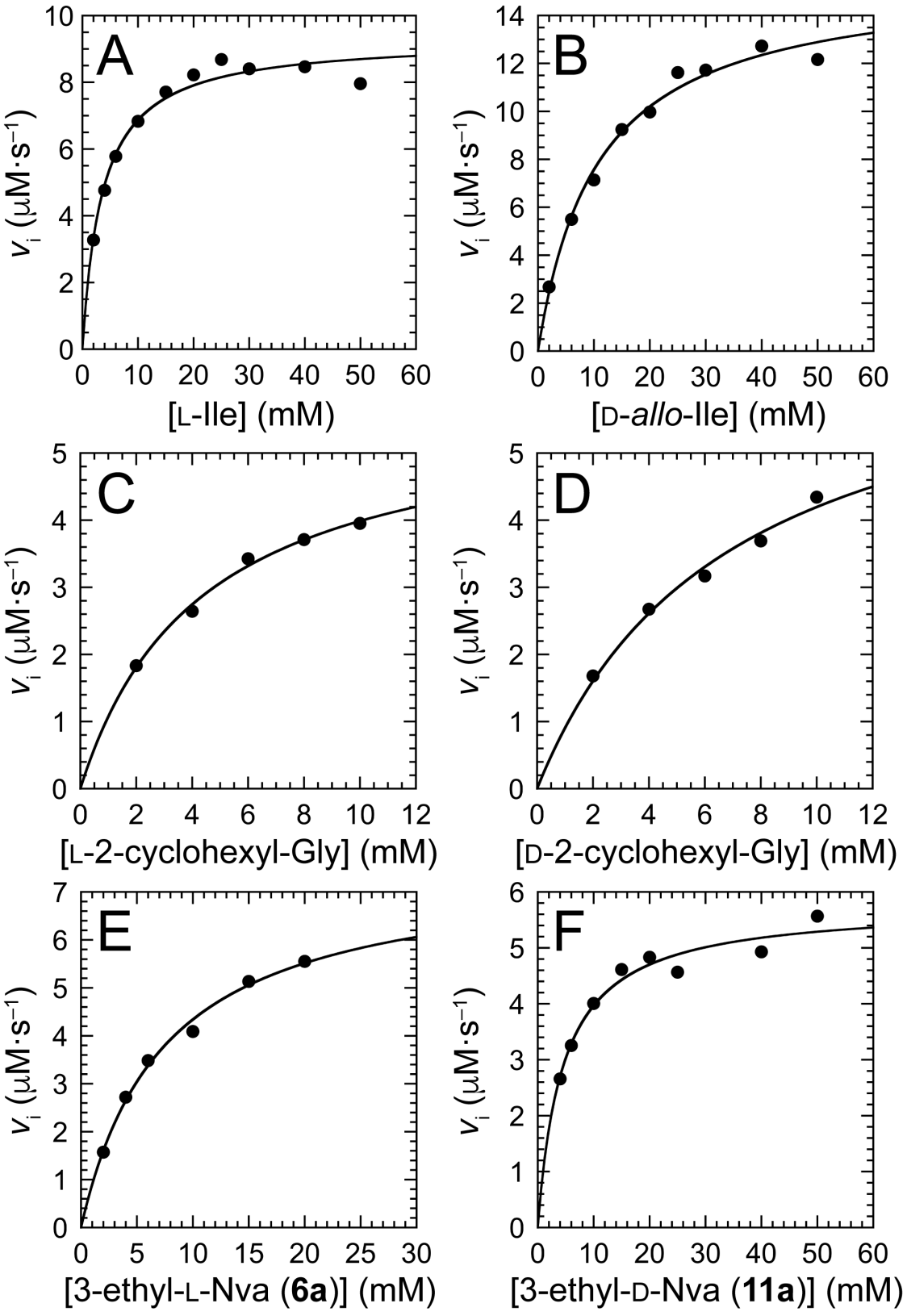
A
B
C
D
E
F
v_i (μM·s^{-1})
[L-Ile] (mM)
[D-*allo*-Ile] (mM)
[L-2-cyclohexyl-Gly] (mM)
[D-2-cyclohexyl-Gly] (mM)
[3-ethyl-L-Nva (**6a**)] (mM)
[3-ethyl-D-Nva (**11a**)] (mM)

Figure S46

Figure S46. Representative Michaelis-Menten plots for the determination of kinetic parameters. The dependence of the initial velocities (v_i) on the concentration of substrate is shown for L-isoleucine (A), D-*allo*-isoleucine (B), L-2-cyclohexylglycine (C), D-2-cyclohexylglycine (D), 3-ethyl-L-norvaline (**6a**) (E), and 3-ethyl-D-norvaline (**11a**) (F). The curves are fits of eqn. 1 to the initial velocity data. See the Experimental section for additional details.

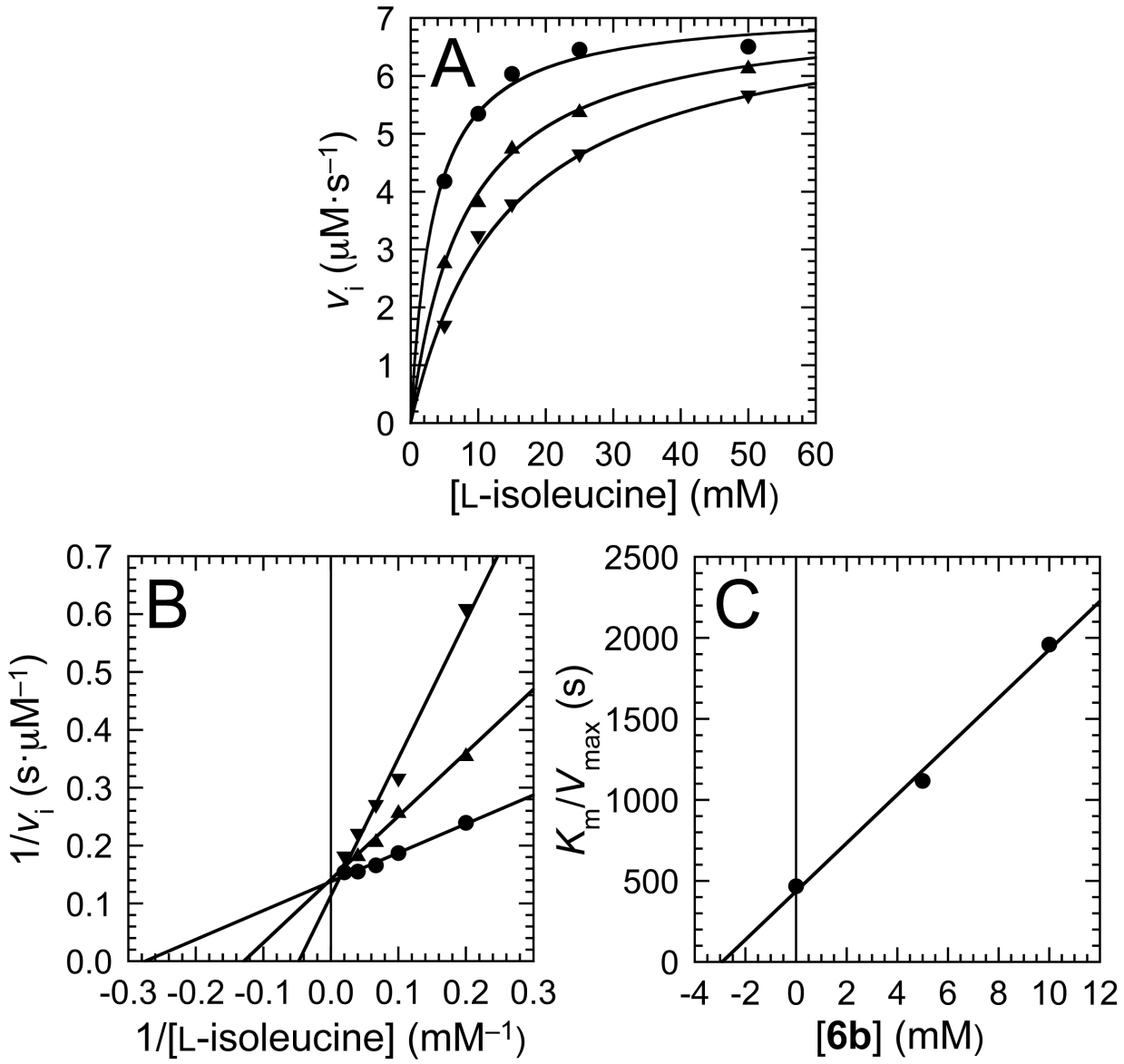

Figure S47. Competitive inhibition of *Lb*IleE by **6b**. A representative Michaelis-Menten plot (A) and Lineweaver-Burk plot (B) showing the competitive inhibition of *Lb*IleE by **6b** are shown. The concentrations of **6b** were 0 (●), 5.0 (▲), and 10.0 mM (▼). The concentrations of the L-isoleucine substrate were 5.0, 10.0, 15.0, 25.0, and 50.0 mM, and the concentration of *Lb*IleE was 2.0 μg/mL. A representative replot (C) of the apparent K_m/V_{max} (values from direct fits of the Michaelis-Menten eqn. 2 to the initial velocity data) vs. inhibitor concentration is shown. The K_i value (determined in triplicate) for inhibition of *Lb*IleE by **6b** is 2.9 ± 0.2 mM.

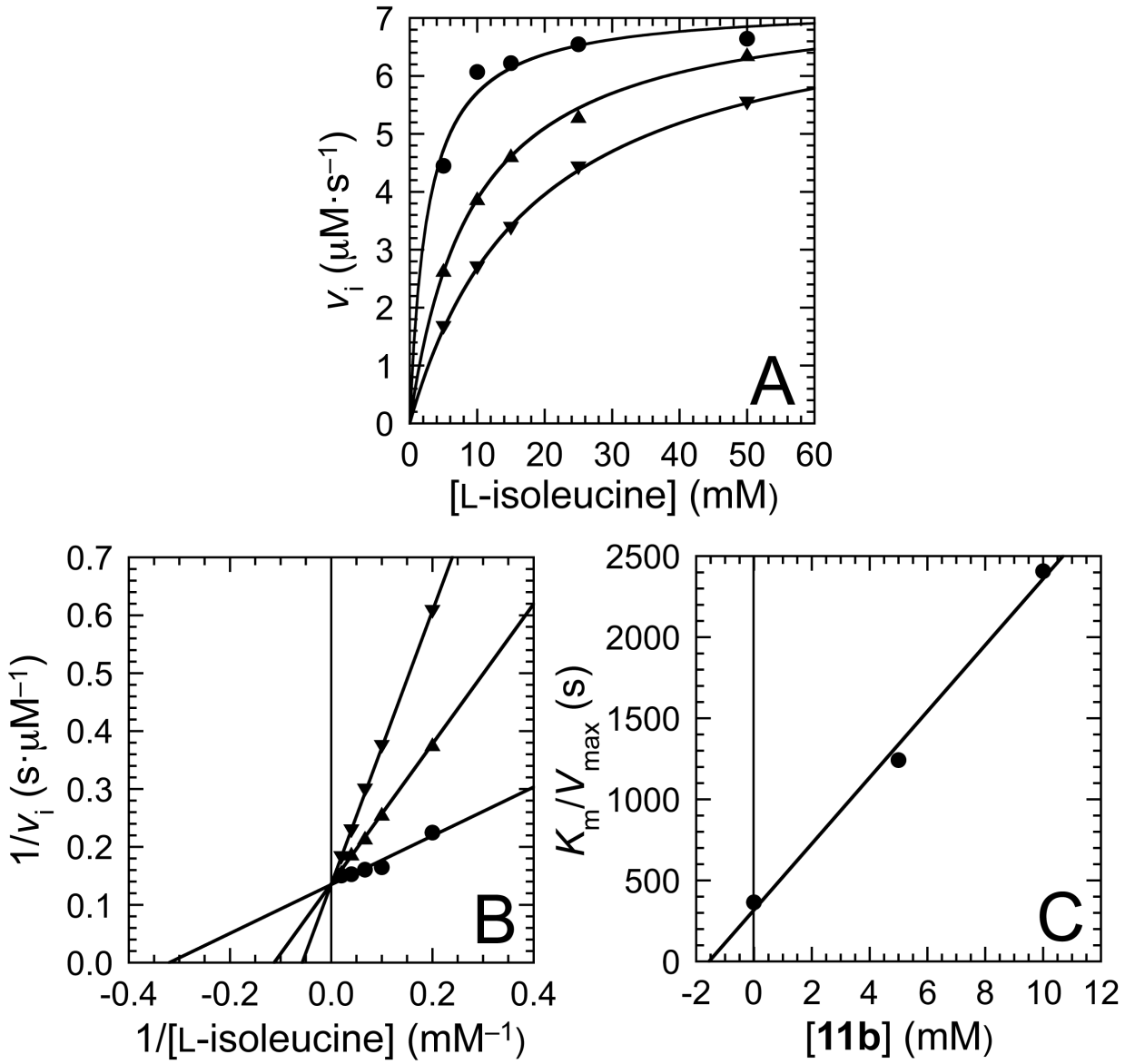

Figure S48. Competitive inhibition of *Lb*IleE by **11b**. A representative Michaelis-Menten plot (A) and Lineweaver-Burk plot (B) showing the competitive inhibition of *Lb*IleE by **11b** are shown. The concentrations of **11b** were 0 (●), 5.0 (▲), and 10.0 mM (▼). The concentrations of the L-isoleucine substrate were 5.0, 10.0, 15.0, 25.0, and 50.0 mM, and the concentration of *Lb*IleE was 2.0 μg/mL. A representative replot (C) of the apparent K_m/V_{max} (values from direct fits of the Michaelis-Menten eqn. 2 to the initial velocity data) vs. inhibitor concentration is shown. The K_i value (determined in triplicate) for inhibition of *Lb*IleE by **11b** is 1.5 ± 0.2 mM.

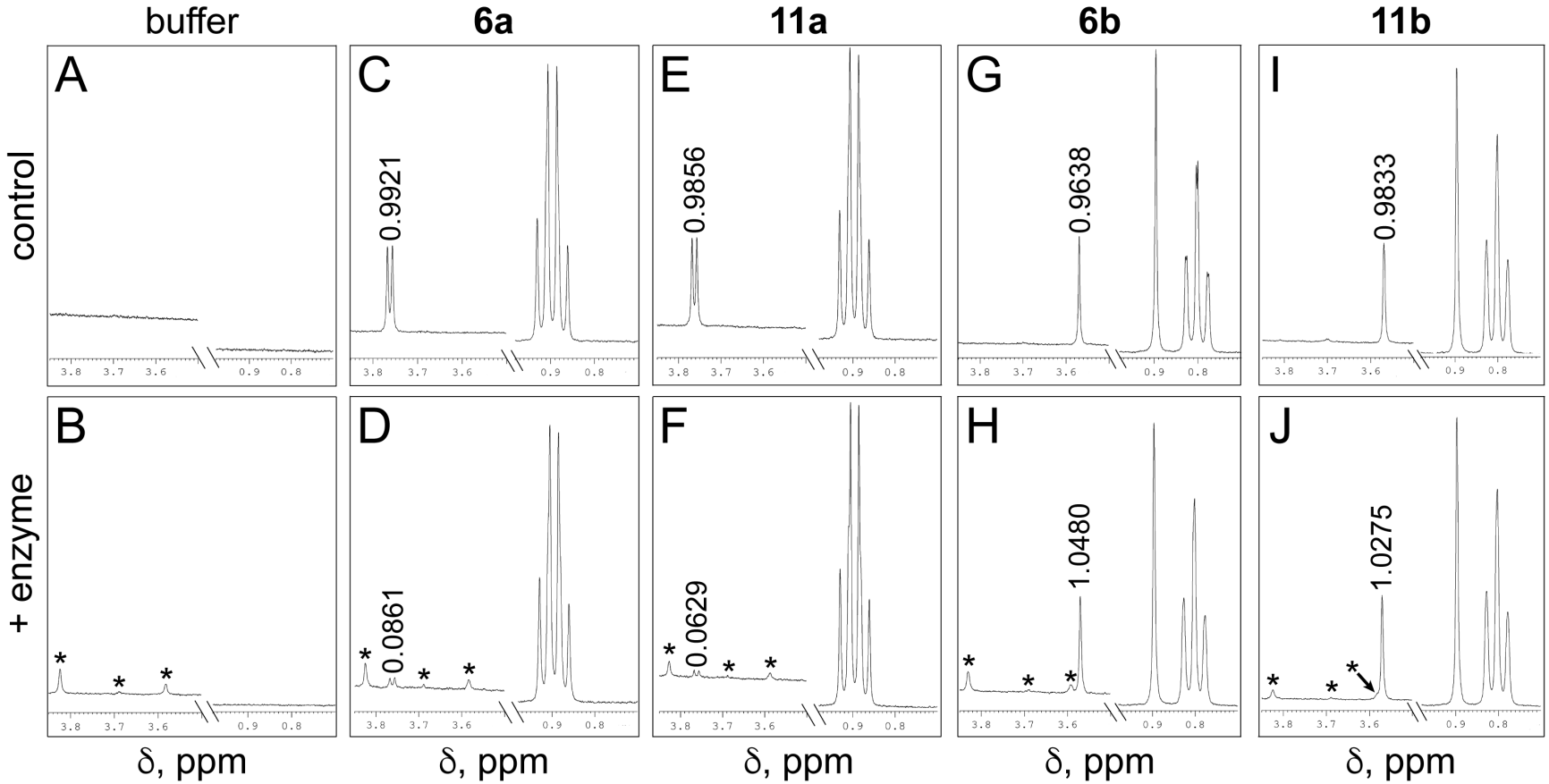
buffer
6a
11a
6b
11b
control
+ enzyme
A
B
C
D
E
F
G
H
I
J
0.9921
0.0861
0.9856
0.0629
0.9638
1.0480
0.9833
1.0275
δ, ppm

Figure S49

Figure S49. *Lb*IleE catalyzes hydrogen-deuterium exchange with **6a** and **11a**, but not **6b** and **11b**. Selected regions of representative ^{1}H NMR spectra are shown. Deuterated assay buffer (200 mM citrate, pD 5.5, containing 0.1 mM PLP) (A) showed the appearance of three signals at 3.82, 3.69, and 3.58 ppm (denoted by *) upon addition of enzyme (B). Over 1 h in the absence of enzyme, the doublet arising from the α-proton of **6a** (C) and **11a** (E) at 3.76 ppm showed no H-D exchange. However, in the presence of enzyme, the doublets showed a marked decrease in signal intensity for both **6a** (D) and **11a** (F), indicating that the α-proton of both compounds had undergone H-D exchange. The integrals are shown above the doublets (3.76 ppm) relative to the overlapping triplets (centered at 0.90 ppm) corresponding to the signal arising from both C$\underline{H}_3$ groups (*i.e.*, 6H). Over 1 h in the absence of enzyme, the singlet arising from the α-proton of **6b** (G) and **11b** (I) at 3.57 ppm showed no H-D exchange. In the presence of enzyme, the singlets showed no significant decrease in signal intensity for both **6b** (H) and **11b** (J), relative to the CC$\underline{H}_3$ (0.90 ppm, 3H) and the overlapping triplets (centered at 0.80 ppm, 6H) corresponding to the signal arising from both $CH_2C\underline{H}_3$ groups, indicating that no H-D exchange occurred at the α-position of both compounds. See the Experimental section for additional details.

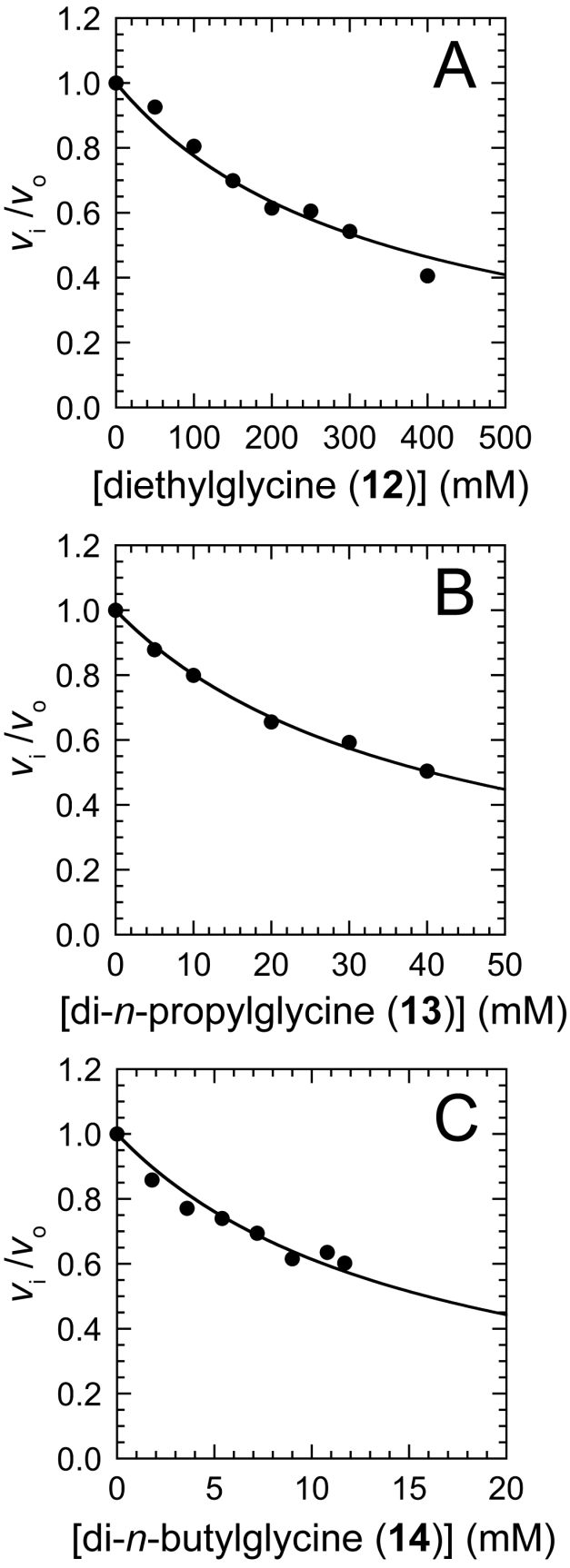
A
v_i/v_o
1.2
1.0
0.8
0.6
0.4
0.2
0.0
0
100
200
300
400
500
[diethylglycine (**12**)] (mM)
B
v_i/v_o
0
10
20
30
40
50
[di-*n*-propylglycine (**13**)] (mM)
C
v_i/v_o
0
5
10
15
20
[di-*n*-butylglycine (**14**)] (mM)

Figure S50. Representative v_i/v_o vs. [inhibitor] plots (IC_{50} curves) for the inhibition of *Lb*IleE by *gem*-dialkylglycines. The curves shown are the nonlinear regression fits of eqn. 3 to the relative velocity values (v_i/v_o). The IC_{50} values for inhibition by 2,2-diethylglycine (**12**), 2,2-di-*n*-propylglycine (**13**), and 2,2-di-*n*-butylglycine (**14**) were 334 ± 18 mM, 43 ± 5 mM, and 16 ± 2 mM, respectively (from three determinations). For compounds **13** and **14**, the IC_{50} values are estimated by extrapolation due to the limited solubility of the compounds in the assay buffer. The concentration of L-isoleucine was 5.0 mM and the concentration of *Lb*IleE was 2.0 μg/mL. See the Experimental section for additional details.

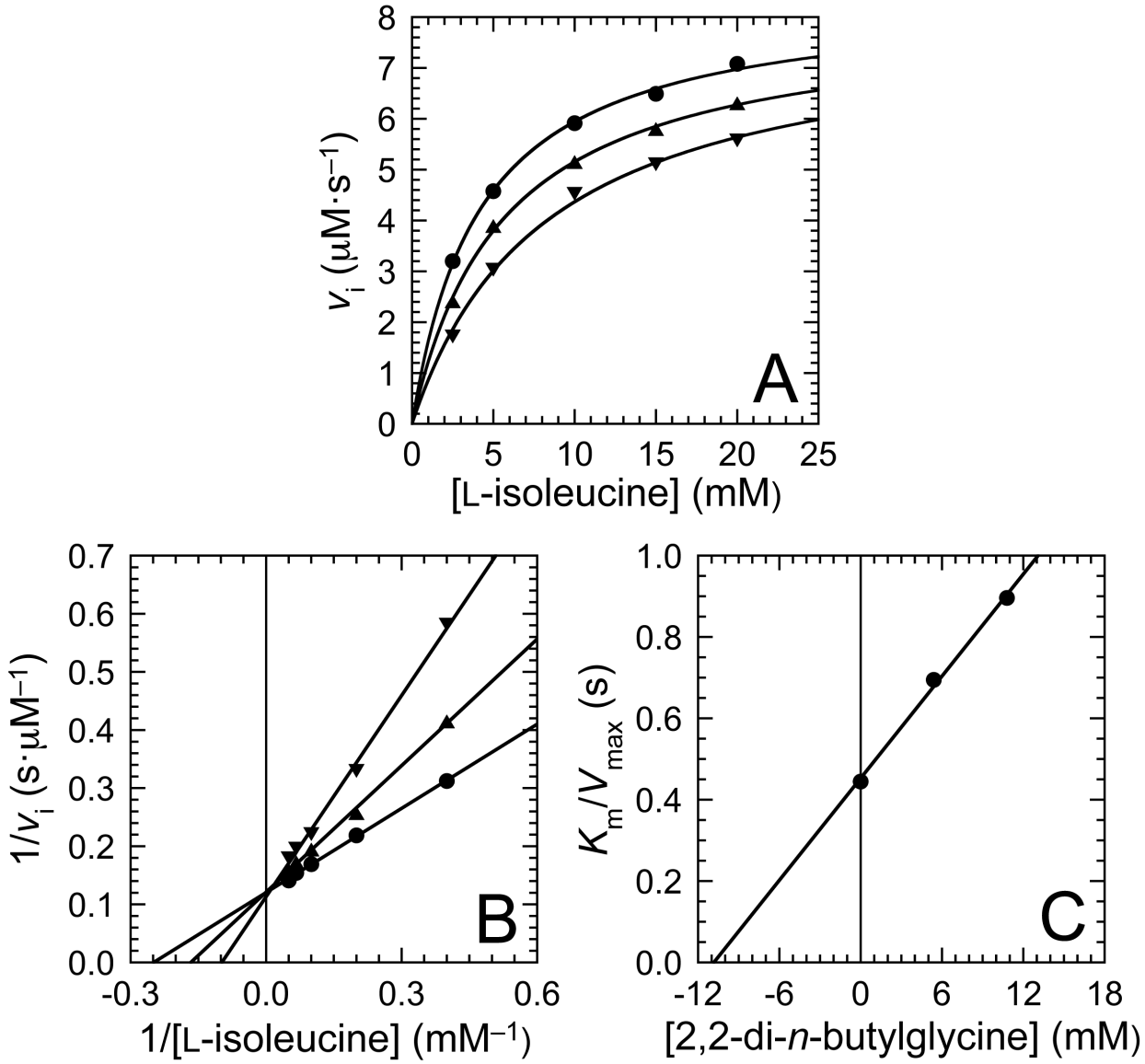

Figure S51. Competitive inhibition of *Lb*IleE by 2,2-di-*n*-butylglycine (**14**). A representative Michaelis-Menten plot (A) and Lineweaver-Burk plot (B) showing the competitive inhibition of *Lb*IleE by **14** are shown. The concentrations of **14** were 0 (●), 5.4 (▲), and 10.8 mM (▼). The concentrations of the L-isoleucine substrate were 2.5, 5.0, 10.0, 15.0, and 20.0 mM, and the concentration of *Lb*IleE was 2.0 μg/mL. A representative replot (C) of the apparent K_m/V_{max} (values from direct fits of the Michaelis-Menten eqn. 2 to the initial velocity data) vs. inhibitor concentration is shown. The K_i value (determined in triplicate) for inhibition of *Lb*IleE by **14** is 11.0 ± 0.2 mM.